EFFECT OF IRON POWDER PARTIALLY USED AS PORTLAND CEMENT REPLACEMENT ON THE STRUCTURAL PROPERTIES OF CONCRETE

MOUSSA ANAN LARGEAU

MASTER OF SCIENCE IN CIVIL ENGINEERING

(Structural Option)

PAN AFRICAN UNIVERSITY

INSTITUTE OF SCIENCE, TECHNOLOGY

AND INNOVATION

2018

DECLARATION

This thesis is my original work and has not been submitted to any educational institution or university for the award of a certificate. Therefore, I declare that all the materials quoted in this thesis, which are not mine have been duly acknowledged.

SIGNATURE:…… DATE…….

MOUSSA ANAN Largeau

This thesis has been submitted with our approval as a university supervisors.

SIGNATURE:…… DATE…….

Prof. Raphael MUTUKU

Civil Engineering Department, Technical University of Mombasa

SIGNATURE:…… DATE……..…….

Dr JOSEPH THUO

Lecturer Dedan Kimathi University of Technology

DEDICATION

This thesis is dedicated to: my endearing wife YANKIMADJI NOUBATA Milka, my beloved beautiful daughter DJANBEYE MANNELOUM Royalty, my great parents NGARHODJINA Anan Gaston and HAMINA ACHENE, my beloved brothers and sisters, my friends who encourage and support me and all the people in my life who touch my heart, thanks for always being there for me, I dedicate this research.

ACKNOWLEDGEMENT

My sincere gratefulness to: African Union Commission (AUC) for the award of scholarship, Japan International Conference Agency (JICA), my main supervisor **Eng. Prof. Raphael MUTUKU**, my second supervisor **Dr Joseph THUO,** my supervisor for corrections **Prof. Christopher Kanali**, Structural and Materials Laboratory of JOMO Kenyatta University of Agriculture and Technology (JKUAT), and all the staff of PAUSTI for their various contributions to the accomplishment of this thesis.

ABSTRACT

Concrete is the most usable material in the construction industry, as a porous material, it is suggested to many chemical attacks. It required to improve its quality during the time using nanoparticles. Nanotechnology offers the possibility of great advances of concrete in construction and can reduce its porosity. The nanotechnology improves the materials bulk properties, controls nanoscale attack on Alkali Silicate Reaction (ASR) and lowers level of environmental attack. Therefore, the use of nanoparticles in the concrete has many benefits. In this research, the iron oxide particles were used in the concrete to investigate the physical and mechanical properties of concrete. The concrete was made using a grade M25 for the mix design and the water-cement ratio was considered varied from 0.500 to 0.526.

In this study, the effect of iron powder (Fe2O3) partially used as cement replacement on the physical and mechanical properties of concrete exposed to chemical attacks was experimentally investigated. For this purpose, Portland cement was partially replaced by 1.5, 2.5, 3.5, and 5% by weighing of iron powder. The workability of the fresh composite concrete was determined using cone Abrams method, mechanical properties were determined included compressive and tensile strengths at 7, 14, and 28 days and durability evaluated by water absorption, permeable porosity, sorptivity, chemical attacks, and chloride penetration. The durability was evaluated by exposing the specimen to sodium chloride and hydrochloric acid for a period of 28, 45 and 60 days. The structural performance was investigated and compared to the traditional concrete with the concrete containing iron powder.

The results showed that the compressive and tensile strengths improved with a certain level of iron powder. However, the maximum value was gained at 2.5 % cement replacement by weight for compressive strength and 1.5% for tensile strength. The workability of the fresh mixtures decreased when iron powder amount increased. It was observed that the porosity decreased respectively by 21.88 and 26.77% at 1.5 and 2.5% replacement.

In terms of durability performance, the results showed that the addition of iron powder lessen the diffusion of chloride ion within the concrete and prevent it from reaching the steel reinforcement. The specimen of all the different mixtures showed more degradation when exposed to 3% hydrochloric acid solution for 28, 45 and 60 days than the one exposed to 2% hydrochloric acid solution.

From result obtained, when 2.5% of iron powder replaced by Portland cement, the flexural strength increased by 18.22% at 28 days for the case of the non-reinforced concrete beam (NRC-B). The reinforced concrete beam (RC-B) with 2.5% of iron powder was judged to be structurally more efficient than the control specimen. Moreover, this present study shows that it is important and benefits to improve concrete properties by using micro-particles materials as a partial replacement of Portland cement.

TABLE OF CONTENTS

LIST OF FIGURES

LIST OF TABLES

LIST OF APPENDICES

ABBREVIATIONS

ACI	American Code Institute
JKUAT	JOMO Kenyatta University of Agriculture and Technology
SEM	Scanning Electron Microscopy
BSI	British Standard Institute
BS EN	British Standard European Norm
ASTM	American Standard of Testing and Materials
AASHTO	American Association of State Highway and Transportation Officials
W/C	The Water/Cement Ratio
OPC	Ordinary Portland cement
UTM	Universal Testing Machine
ASR	Alkali-Silica Reaction
OH^-	Hydroxyl ions
Na^+	Sodium ions
K^+	Potassium ions
Fe_2O_3	Iron (III) oxide / Hematite
Fe_3O_4	Iron (II, III) oxide / Magnetite
NaCl	Sodium chloride
HCl	Hydrochloric acid
SiO_2	Silicon dioxide / silica
$Ca(OH)_2$	Calcium hydroxide
ZrO_2	Zirconium dioxide

C_3S or $(CaO)_3\ SiO_2$	Tricalcium silicate
C_2S or $(CaO)_2\ SiO_2$	Dicalcium silicate
Al_2O_3	Aluminum Oxide / Alumina
TiO_2	Titanium dioxide
ZnO	Zinc oxide
CO_2	Carbon dioxide
NS	Nano silica
NA	Nano alumina
NF	Nano iron oxide
C_3A	Tricalcium alumina
C_4AF	Tetracalcium aluminferrate
MgO	Magnesium oxide

SYMBOLS

A	Mass of the oven-dried sample in air (g)
B	Mass of the surface-dry sample in the air after immersion (g)
C	Mass of the surface-dry sample in the air after immersion and boiling (g)
D	Apparent mass of sample in water after immersion and boiling (g)
$\boldsymbol{g_1}$	Bulk density, dry (g/cm^3)
$\boldsymbol{g_2}$	Apparent density (g/cm^3)
$\boldsymbol{\rho}$	Density of water (g/cm^3)
S	Slump (mm)
P	Content of iron powder (%)
Cf	Compaction factor
Wai	Water after immersion
Waib	Water after immersion and boiling
Wa	Water absorption
Fc	Compressive strength (MPa)
n	the porosity (%)
Ft	tensile splitting strength (MPa)
E	Modulus of elasticity (Young's Modulus)

I	Moment of inertia
Ø	Curvature
y	Compression depth of the section
v	Poisson’s ratio
e	Strain
ξ	Principal strain
σ	Stress

CHAPTER ONE

1. INTRODUCTION

1.1 Background to the Study

Concrete is a very important building material used in construction. Even though it gives the impression to be well known and its behavior is usually understood, there is still several research project carrying out in order to investigate it on physical, mechanical properties and its microstructural level.

The understanding of the structure and behavior of concrete at the fundamental stage is a necessary and very appropriate use of nanotechnology. One of the fundamental aspects of nanotechnology is its interdisciplinary nature (Soleymani, 2012). The use of concrete in constructions and buildings may have begun less than a century ago. However, the increasing of the use of concrete from decade to decade has led, much more recently, to extensive and effective research in improving the properties of concrete, incorporating a wide range of supplementary cementing materials, such as pozzolans and nanoparticles. Recently, nanotechnology has attracted widespread scientific attention because of the new potential uses of particles at the nanometer (10−9 m) scale. This may be due to the fact that nanoscale-size particles are able to significantly improve properties compared with grain-size materials of the same chemical composition (Arefi et al., 2012). Previously, several works have been conducted on concrete composites by adding different nanoparticles evaluating the mechanical properties of concrete. The activity of nanoparticles can act as heterogeneous nuclei for cement pastes, further accelerating cement hydration, as Nano-reinforcement, and as Nano-filler, densifying the

microstructure, leading to a reduced porosity (Ahmed et al., 2015). Even though certain nanomaterials have been extensively studied, there is still a high amount of available nanomaterials which influence the properties of concrete which still need to be investigated. One of the most promising nanomaterials which should be further investigated is nano-Fe_3O_4 (nano-magnetite). The studies related to the application of iron oxides (especially Fe_2O_3) in cementitious composites have shown that these nanomaterials positively influence the mechanical and microstructural properties by improving compressive and flexural strength and by reducing the total porosity of the composites (Sikora et al., 2016). Various mineral additives such as fly ash and silica fume have been traditionally utilized in cement composites not only for their environmental and economic advantages but also for their technical benefits such as the ability to fill in micro and macro-voids and displaying partial binder effect. On the other hand, a significant increase is observed over the past few years in the number of studies about the utilization of nano-sized materials in cement composites. Nano-powders are expected to influence the kinetics and hydration of cement significantly and yield better results in filling of voids of cement-based composites compared to the mineral additives due to their larger surface area and greater electrostatic force (Oltulu et al., 2013). When Ferrite nanoparticles are added to cement/concrete, they act as filler to fill the pores between cement particles resulting in finer pore structure. Also, the more C-S-H gel can be formed in concrete due to the reaction that occurs between the Ferrite nanoparticles and the $Ca(OH)_2$ in the hydrating of cement (Ahmed et al., 2015).

The durability of a concrete structure largely dependent on the possibilities of ingress water, gases, and ions into the porous material. The size of the pores, of micro-cracks and

their connectivity, the nature of the phases and their reactivity with the various chemical are the most important parameters controlling penetration of external agents (Ollivier et al., 1992). Degradation of concrete members exposed to aggressive sulfuric acid environments is a key durability issue that affects the life cycle performance and maintenance costs of vital civil infrastructure. Sulfuric acid in groundwater, chemical waste or generated from the oxidation of sulfur-bearing compounds (e.g., pyrite) in backfill can attack substructure concrete members. The effect of sulfuric acid on concrete is more detrimental than that of sulfate attack; in addition to attack by sulfate ions, there is a dissolution effect caused by hydrogen ions (Bassuoni & Nehdi, 2007). The alkali-silica reaction (ASR) is caused by the presence of reactive aggregates in contact with sufficiently alkaline pore solution and a moisture level above 80%, which leads to the formation of expansive products that cause cracking and deterioration of the structures (Ponce et al., 2006). The first stage of the alkali-silica reaction is the reaction between the hydroxyl ions (OH^-) in the pore solution and reactive silica in the aggregate; the silica is not directly attacked by the alkali metal cations (Na^+ and K^+). The alkalis contribute initially to the high concentration of hydroxyl ions in solution and later to the formation of an expansive alkali-silica gel. The amount of expansion and resulting damage that occurs in concrete affected by alkali-silica reaction depends on a number of parameters including the availability of alkalis in the system, the nature and amount of reactive silica in the aggregate, exposure conditions (temperature and moisture availability) and the degree of internal and external restraint to movement (e.g., amount and distribution of reinforcing steel) (Thomas, 2011). Pores in concrete can also result from inadequate compaction. This pore system governs the most important properties of concrete, notably

its strength. Well-compacted concrete prepared with hard low-porosity aggregates may be assumed to be a multiphase material consisting of coarse aggregates embedded in a mortar matrix (Kumar et al., 2003).

A broad range of challenges faced by the construction industry, ranging from the performance of the materials to environmental and safety issues, relate to materials and their properties. Recent developments in various areas of nanotechnology show significant promise in addressing many of these challenges. Research and development have demonstrated that the application of nanotechnology can improve the performance of traditional construction materials, such as concrete and steel. Noteworthy improvements in concrete strength, durability and sustainability are being achieved with the considered use of metal oxide nanoparticles and engineered nanoparticles (carbon nanotubes and carbon nanofibers). Nanotechnology has the potential to reduce the environmental impact and energy intensity of structures, as well as improve safety and decrease costs associated with civil infrastructure (Hanus et al., 2013).

The aim of this present study is to incorporate iron powder (Fe_2O_3) particles into normal concrete to examine physical and mechanical properties and chemical attacks of concrete. Several specimen with a various amount of iron powder (1.5, 2.5, 3.5 and 5%) were prepared and their physical and mechanical properties were measured for different partial replacement of Fe_2O_3 particles to the concrete paste.

1.2 Statement of the Problem

Concrete has a highly heterogeneous and complex microstructure. It is a porous material susceptible to several external attacks that can affect its durability. Consequently, in multiphase materials such as concrete, the porosity of each component of the microstructure can become strength-limiting. It was recognized long ago that the reduction of the porosity increases the strength of the solid materials in general and the strength of cement-based materials in particular. It has been also discovered that the porosity plays an important role in the frost resistance of concrete. Furthermore, porosity has a role in the relationship between mechanical properties of concrete, such as the compressive strength-modulus of elasticity relationship (Chen et al., 2013).

Concrete is the most widely used construction material in the world, up to 10 billion tons per year worldwide consumption. Deterioration is any adverse change of normal, mechanical, physical, and chemical properties either in the surface or in the body of concrete, generally due to the disintegration of its components. Degradation processes of concrete usually start from the materials level and then proceed to the structural level. (Zongjin et al., 2009). Degradation of concrete members exposed to external attacks is the main cause of durability issue that affects the life cycle performance and maintenance costs of vital civil infrastructure. The durability issue comes also from the result of inadequate compaction of concrete which increases pores in the concrete member.

Therefore facing these problems of environmental attack, there is the need to make concrete which is less porous and with high performance. The iron powder will be used in this research to reduce the pores in concrete and to improve the life cycle performance of concrete and reduce the maintenance costs of structures. The present study is focused

on the structural changes on concrete when adding nano-Fe_2O_3 as admixtures in different percentages.

1.3 Objectives

1.3.1 General objective

The general objective of this project is to investigate the effect of iron powder partially used as cement replacement on structural properties of concrete and durability performance.

1.3.2 Specific objectives

1. To assess the physical and chemical properties of iron powder, Portland cement and aggregates.
2. To determine the influence of iron powder on the physical and mechanical properties of concrete.
3. To assess the effect of chemical attack on the durability of concrete with iron powder partial replacement of cement.
4. To evaluate the structural performance of concrete beams made with cement partially replaced with iron powder.

1.4 Justification

The main target of this study was to investigate the effect of iron powder on concrete properties and the degradation of the concrete members when exposed to external attack. To minimize the porosity on the concrete members by using iron powder as a concrete component. The microparticles will reduce the pores on concrete and increase the strength, durability, and sustainability of buildings and infrastructures.

Scanning Electron Microscopy study of the microstructures between the cement mortar mixed with the nanoparticles and the plain cement mortar showed that the nano-Fe_2O_3 and nano-SiO_2 filled up the pores and reduced $Ca(OH)_2$ compound among the hydrates. These mechanisms explained the supreme mechanical performance of the cement mortars with nanoparticles (Li et al., 2004). Therefore, it is feasible to add nanoparticles to improve the mechanical properties of concrete.

Recently, renovation engineering has attracted increasing international attention because of the frequent occurrence of serious degradation of buildings and infrastructures. It is important to understand the basic causes and mechanisms of the various forms of deterioration that degrade construction material and infrastructure made of reinforced concrete. Deterioration of concrete can be caused by a chemical attack from external sources or between the internal materials of which the structure is built, or by physical deterioration due to climatic changes, abrasion, fire, impact, explosion, earthquake, foundation failure or overloading (Zongjin et al., 2009).

Hence the study was focused on the use of microparticles of iron powder to mitigate the permeability of concrete, enhance the concrete properties, improve the structural performance and, improve the issue that affects the life cycle performance and maintenance costs of vital civil infrastructure.

1.5 Scope

The main scope of this study was to investigate the influence of iron powder (Fe_2O_3) on structural properties of concrete. In addition, to mitigate the external attack such as acid attacks and chloride ingress. Various tests will be conducted throughout the study, regarding physical and mechanical properties, as well as durability performance. Finally,

construction of model beams made with the material specimen under study in the laboratory, and tested under four-point loads bending, is one of our important targets. It will help to analyze deeply the structural responses of the materials.

CHAPTER TWO

2. LITERATURE REVIEW

2.1 Theoretical Background

2.1.1 Preview

Nanotechnology refers to the understanding and manipulation of materials on the nanoscale size ($1.0x10^{-9}$m). At the nanoscale, substance properties are dictated by quantum mechanics, Surface effects, rather than bulk properties, dominate. This can lead to marked changes in material properties and can result in improved performance and new functionality. Nanotechnology has broad-reaching applications in the construction industry. Nanotechnology may improve the primary properties of traditional construction materials (e.g., concrete). Nanotechnology has the potential to reduce the environmental impact and energy intensity of structures, as well as improve safety and decrease costs associated with civil infrastructure (Hanus et al., 2013).

Due to a nanoscales size, nanoparticles display unique physical and chemical properties different from those of the conventional materials. Because of their unique properties, nanomaterials have been gaining increasing attention and been applied in many fields to make new products with novelty functions. Among all nanoparticles, the carbon nanotube composites are the most abstracting (Li et al., 2004). Besides many oxide nanomaterials like nano-SiO_2, nano-TiO_2, nano-Fe_2O_3, nano-Al_2O_3, nano-ZrO_2, Nano-cement particles of C2S (Alita) and C3S (belite), and Nano-clays have been tested, those improve the cement-based materials performance (Mendes et al., 2015).

2.1.2 Nanoparticles for construction

a) The carbon nanotubes

Carbon nanotubes are a form of carbon having a cylindrical shape, the name coming from their nanometer diameter. They can be several millimeters in length and can have one "layer" or wall or more than one wall (Olar, 2011). Nanotubes are members of the fullerene structural family and show extraordinary strength and unique electrical properties, being efficient thermal conductors. For example, they have five times Young's modulus and eight times (theoretically 100 times) the strength of steel, whilst being 1/6th the density. Expected benefits of carbon nanotubes are: mechanical durability and crack prevention in concrete, improved mechanical and thermal properties in ceramics and real-time structural health monitoring capacity (Mann, 2006).

b) Titanium dioxide nanoparticles

The nanoparticles of dioxide of titanium are added to the concrete to improve its properties. This white pigment is used as a layer thoughtful reflected or added in paints, cement, and windows for its properties of sterilization. The dioxide of titanium demolishes organic pollutants, compounds organic volatile and bacterial membranes by powerful photocatalytic reactions, reducing air pollutants when it is applied to the outside surfaces. Being hydrophilic gives self-cleaning properties to the surfaces to which it is applied because the rainwater is attracted to the surface and forms sheets which gather the pollutants and dirt particles previously demolished and washes them off. The resulting concrete surface has a white color that retains its whiteness very effectively (Mann, 2006).

c) Silicon dioxide nanoparticles

The dioxide of silicon (SiO_2) could increase significantly the compressive strength of concretes enveloping large fly ash volume at an early age, by filling the pores between large fly ash and cement particles. Nano- SiO_2 decreases the setting time of mortar when compared with silica fume (micro-silica) and reduces bleeding water and segregation by the improvement of the cohesiveness (Sadrmomtazi et al., 2010).

d) Iron oxide nanoparticles

Although copper, cobalt, and nickel are highly magnetic materials, they have very limited applications due to their toxicity and susceptibility to oxidation. Unlike these, iron oxide nanoparticles have attracted extensive interest due to their superparamagnetic properties and their potential uses in many fields (Rattan et al., 2016).

Even though certain nanomaterials have been extensively studied, there is still a high amount of available nanomaterials which influence the properties of concrete still need to be revealed. One of the most promising nanomaterials which should be further investigated is nano-Fe_3O_4 (Nano-magnetite). The studies related to the application of iron oxides (especially Fe_2O_3) in cementitious composites have shown that these nanomaterials positively influence the mechanical and microstructural properties by improving compressive and flexural strength and by reducing the total porosity of the composites (Oltulu et al., 2013). In addition, the application of nano-Fe_2O_3 can be very beneficial in improving the self-sensing properties of concretes (Han et al., 2014).

e) Zinc oxide nanoparticles

Zinc oxide is a unique material that exhibits semiconducting and piezoelectric dual properties. It is added to various materials and products, including plastics, ceramics,

glass, cement, rubber, paints, adhesives, sealants, pigments, fire retardants. Used for concrete manufacturing, ZnO enhances the processing time and the resistance of concrete against water (Broekhuizen et al., 2009).

f) Aluminum oxide nanoparticles

Aluminum oxide (Al_2O_3) component reacts with calcium hydroxide produced from the hydration of calcium silicates. The rate of the pozzolanic reaction is proportional to the amount of surface area available for reaction. The addition of nano-Al_2O_3 of high purity improves the characteristics of concretes, in terms of higher split tensile and flexural strength. The cement could be advantageously replaced in the concrete mixture with nano-Al_2O_3 particles up to maximum limit of 2.0% with average particle sizes of 15 nm, the optimal level of nano-Al_2O_3 particles content being achieved with 1.0% replacement (Nazari et al., 2010).

g) Zirconium oxide nanoparticles

Zirconium oxide nanoparticles are white high surface area particles with typical dimensions of 5 to 100 nanometers and the specific surface area in the 25 to 50 m^2 /g range. Nano zirconium shows good aesthetics, superior physical resistance (hardness, flexibility, and durability), and chemical resistance (practically inert) and is a very good insulator. (Olar, 2011).

2.1.3 Applications of iron oxide

The use of hematite and other iron oxides as natural red ceramic pigments has been practiced since prehistoric times. The iron oxides such as magnetite, hematite, magnetite, and goethite are commonly used as pigments for black, red, brown and yellow colours respectively. Predominantly natural red iron oxides are used in primers for steel

constructions and cars reducing corrosion problems. World consumption of iron oxide pigments comprises 63% in synthetic form and 37% from natural resources. The construction sector – roof tiles, paving slabs and other concrete products – accounts for a major chunk of total world consumption. By reducing the particle size to nano range, transparent iron oxide pigments can be obtained. The manufacturing process of transparent iron oxide pigments depends on the control of physical and surface chemistry properties. Particle size is optimized to ensure that minimal light interference occurs thus maximizing transparency. In general particle size from 2 to 10 nm increases transparency 3-10 times when compared to the bulk form (Elizabeth, 1992). Nowadays such transparent iron oxide pigments are preferably used. These have good stability to temperature, the red can resist up to 3000˚C while the yellow, black, green and brown can withstand up to 1600˚C. These are strong absorbers of ultraviolet radiation (Sreeram et al., 2006) and mostly used in automotive paints, wood finishes, construction paints, industrial coatings, plastic, nylon, rubber, and printer ink. The excellent weather fastness, absorption properties, high transparency, and color strength makes trans-oxide to enrich the colors, increase color shades when combined with organic pigments and dyes (Mohapatra et al., 2010).

2.2 Experimental Background

Sikora1 et al. (2016), carried out an experimental study of the effect of nano- Fe_3O_4 as an admixture on the mechanical and microstructural properties of cementitious. It showed that Fe_3O_4 nanoparticles acted as a filler which improved the microstructure of a cementitious composite and reduces its total porosity, thus increasing the density of the composite. The presence of nano-magnetite did not affect the main hydration products

and the rate of cement hydration. In addition, the samples containing Nano-magnetite displayed up to 20% the compressive strength improvement. The study showed that 3% of nano-Fe_3O_4 in the cementitious composite was the maximum amount to improve both its mechanical and microstructural properties. In the presence of nano-Fe3O4, a positive effect on the microstructure of the cementitious composite is noticeable; however, exceeding a certain limit might lead to the creation of local agglomerations of magnetic nanoparticles, which might not be beneficial for the mechanical response of the cement matrix (Sikora et al., 2016).

The following conclusions were drawn: nano magnetite additive does not affect the consistency of the fresh mortars when it is applied up to 5 % by weight of cement; nano magnetite can act as a filler of the microstructure of cement pastes by refining the pore structure and reducing the total porosity, thus increasing the density of the composite; Fe3O4 nanoparticles can be successfully applied as an admixture for cementitious materials and its presence does not affect the rate of the cement hydration and the nature of the phases in hydrated cement paste; nano-Fe3O4 particles have a tendency towards agglomeration; therefore, high amounts of the admixture might lead to local agglomerations and microcrack formation, what is responsible for a deterioration in the mechanical properties of cement-based composites; and there is a certain amount of nano-Fe3O4 (3%) which can be beneficial for the properties of cementitious composites. Exceeding this limit might lead to a neutralization of the positive effect of the nanoparticles.

Mohamed et al. (2015) in their work conducted on the effect of incorporation of ferrite nanoparticles on compressive strength and resistivity of self-compacting concrete (SCC)

found that concrete specimen reinforced with $MnFe_2O_4$ nanoparticles had higher compressive strength compared to that of the concrete without $MnFe_2O_4$ nanoparticles. It was found that the cement could be advantageously doped with $MnFe_2O_4$ nanoparticles up to maximum limit of 1% by weight of cement with an average diameter of 49 nm. However, the maximum value of compressive strength was achieved with 0.5 % by weight doped $MnFe_2O_4$ nanoparticles. The addition of $MnFe_2O_4$ nanoparticles with 1.5 and 2 % (by weight) led to a compressive strength lower than the control specimen. The pore structure of self-compacting concrete containing $MnFe_2O_4$ nanoparticles was improved and the volume of all mesoporous and macro pores was decreased. SEM images showed that specimen reinforced with $MnFe_2O_4$ nanoparticles with 0.5 % by weight was more compact and less porous in the paste with admixture than the control one (Ahmed et al., 2015)

Rahmat et al. (2015) carried out an experimental investigation on the durability of self-compacting mortar containing nano-SiO_2, nano-Fe_2O_3, and nano-CuO, and their findings showed that there is enhancement by using nanoparticles in the cementitious paste. In the study, the durability properties of self-compacting mortar (SCM) incorporating nano-SiO_2, nano-Fe_2O_3 and nano-CuO were experimentally compared with that of plain mortar. Portland cement was partially replaced by 25% fly ash and three different nanoparticles by up to 5 %. The amount of water-binder ratio and cementitious materials content were considered constant. mechanical characteristics were determined included compressive strength at 3, 7, 28 and 90 days and durability evaluated by water absorption, electrical resistivity and rapid chloride permeability test (RCPT). The microstructure of the mortars was also assessed via scanning electron microscopy (SEM).

It was observed that the workability increased slightly and also nanoparticles could improve the mechanical and durability properties of SCM specimen. The SEM micrographs illustrated more packed pore structure of the mortars containing nanoparticles which leads to increase in strength and durability of SCM specimen (Madandoust et al., 2015).

The study was conducted to assess the effect of nanoparticles on the properties of self-compacting mortar. The following conclusions were drawn: incorporation of nanoparticles made the mortars more viscous. The rheological properties of specimen with the addition of different nanoparticles altered slightly; the compressive strength of the specimen is increased by using up to 4 % NS, 2 % NF and 3 % NC (by weight) and then it is decreased. The water absorption of the specimen is decreased by increasing the nanoparticles content. Electrical resistivity results showed significant enhancement by addition of nanoparticles; the chloride permeability values decreased by 60%, 44% and 44% by addition of NS, NF, and NC, respectively. According to the SEM micrographs, smaller pores achieved by the addition of nanoparticles, which can improve the mechanical, durability and microstructural properties of the SCMs mixtures.

Oltulu et al. (2013) carried out an experimental comparative study of the effect of nano-SiO_2 (NS), nano-Al_2O_3 (NA) and nano-Fe_2O_3 (NF) powders on compressive strengths and capillary water absorption of cement mortar containing fly ash (FA). It was reported that the addition of only one type of oxide powders at 1.25% enhanced compressive strength of the mortars much further than the other proportions. The use of NS + NA powders at 1.25% increased the compressive strength by the most compared to the control specimen. For all binary powder combinations, the rate of increase in strength reached generally

their peak on the 28th day and gradually decreased through aging. Among all groups, the best results were obtained from the mortars added with NS + NA + NF powders at 1.25%. For this particular mortar, 7 to 32% increase in the compressive strength and 14% decrease in the capillary absorption were determined relative to the control specimen. (Oltulu et al., 2013).

The conclusions made from the study could be summarized as follows: NS powder affected the specimen prepared with FA in a similar way with SF added specimen. Addition of this powder at 1.25% increased the compressive strength of mortars with FA much further compared to the other proportions, especially at early ages. The proportion of 2.5% lead to a decrease in strength values. The use of 1.25% NS + NA powders improved the compressive strength by the most compared to the control specimen. The facilitation of pozzolanic reactivity by binary powder combinations more strongly at certain time intervals. Nonetheless, detailed investigations should be conducted in order to determine the factors resulting in mortars such as fluctuations in strength values. For the mortars containing FA, if the use of a single type of Nanopowder is compared to that of binary combinations, it can be seen that the best results were obtained from specimen 1.25 NS and 0.5 NAF. Therefore, the use of NA + NF binary combination at a proportion of 0.5% (0.5 NAF) is sufficient to obtain the desired strength improvement. Besides, the use of less amount of Nanopowder is not only beneficial for preventing the agglomeration of powders in the mixture but also it is desirable from the economic point of view.

The decline in early age strength observed in groups containing SF and binary powder combinations was not encountered in similar mortars containing FA. The mortar 0.5 NS

is an exception to this observation. The binary powders yielded better results with respect to the capillary absorption in SF added mortars compared to FA-containing mortars. Among the mortars containing ternary combinations of FA, the highest strength improvement was displayed by 1.25% addition of Nanopowders which also reduces the capillary absorption by the most. On the other hand, among all groups containing FA (single type, binary and ternary), the best physico- mechanical result was obtained from the mortars containing 1.25% NS + NA + NF powders.

Branch et al. (2011) in their study conducted on the effect of adding Fe_2O_3 nanoparticles on the morphology properties and microstructure of cement mortar has been shown once again the useful of using Fe_2O_3 particles as partial replacement of cement. The study has been done on the compressive and tensile strength of cement mortar containing Fe_2O_3 nanoparticles in the amounts of 1, 3 and 5% by weight of cement. The results showed that the mechanical properties of samples containing 1% and 3% Fe_2O_3 nanoparticles are desirable than the ordinary cement mortar. SEM study about the microstructure of cement mortar containing nanoparticles and ordinary cement mortar showed that nano-Fe_2O_3 fills the pores completely and reduces the large crystals of $Ca(OH)_2$ and the hydrate products are denser and compact. The mechanical properties results showed that by increasing Fe_2O_3 nanoparticles up to 5% reduces the mechanical properties.(Branch et al., 2011).

Nazari et al. (2010), carried out on the benefits of Fe_2O_3 nanoparticles in concrete mixing matrix and it was found that there was an improvement of using iron oxide particles as partial replacement of cement in concrete. The purpose of this study was to investigate the compressive strength and workability of concrete by partial replacement of cement with Nano-phase Fe_2O_3 particles. Fe_2O_3 nanoparticles with the average diameter of 15

nm were used with four different contents of 0.5, 1.0, 1.5 and 2.0% by weight of cement. The results showed that the use of nano-Fe_2O_3 particles up to a maximum replacement level of 2.0% produces concrete with improved strength. However, the ultimate strength of concrete was gained at 1.0% of cement replacement. The workability of fresh concrete was decreased by increasing the content of Fe_2O_3 nanoparticles. It is concluded that partial replacement of cement with nanophase Fe_2O_3 particles improves the compressive strength of concrete but decreases its workability.

2.3 Research Gaps

Most researches have been done by adding nanoparticles to improve the mechanical and physical properties. Most of them have been reported on nano-SiO_2, carbon nanotube and nano-Al2O3 in cement-based materials. However, the influence of others nanoparticles, such as nano-CuO, nano-ZnO_2, nano-Fe_3O_4, nano-Fe_2O_3 on the physical and mechanical properties of cement-based materials was also investigated in a few types of research. Many of the studies have been investigated on the use of nanotechnology in the concrete, but the influence of these nanoparticle has not been done fully when it comes to durability and structural performance. In this study, the effect of the iron powder (Fe_2O_3) on physical and mechanical properties and durability performance of concrete will be investigated. Finally, structural performance analysis through beams realized and tested under four-point load bending, will help to understand and well characterized the composite concrete material developed. Some basic important parameters need to be analyzed such as the first crack and failure load, the failure mode and crack patterns, the mid-span deflections, the ultimate moments and curvatures, the flexural stress-strain behaviors, the concrete stress-strain distributions, and steel strains distribution.

2.4 Conceptual Framework

The conceptual framework used in this study is presented in Figure 2.1.

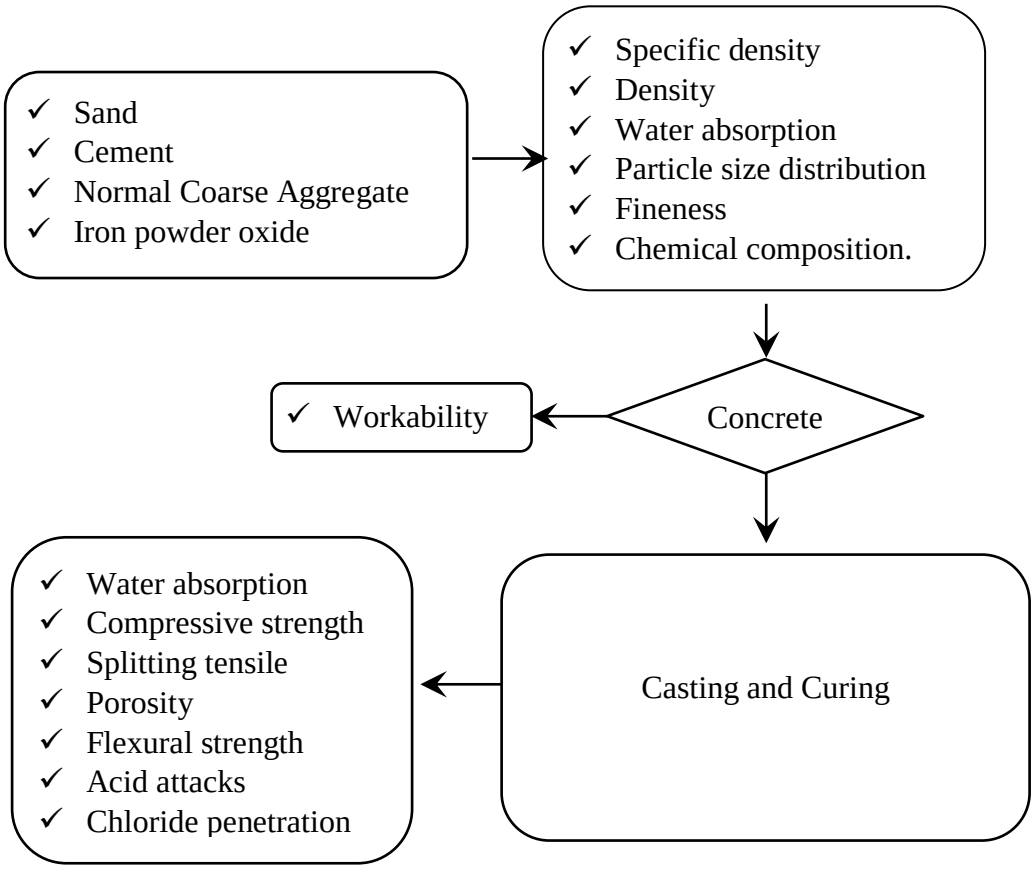

Figure 2-1: Conceptual framework.

CHAPTER THREE

3. MATERIALS AND METHODS

3.1 Materials and Preparation

Concrete is a composite material composed of coarse aggregate bonded together with a fluid cement that hardens over time. When aggregate is mixed together with dry Portland cement and water, the mixture forms a fluid slurry that is easily poured and molded into shape. The cement reacts chemically with the water and other ingredients to form a hard matrix that binds the materials together into a durable stone-like material that has many uses. The most important parameters are the water-cement ratio; cement type; blending agents; cement content; and additives and admixtures. The concrete composition is adapted to the environmental conditions (micro-climate at the concrete surface).

3.1.1 Cement

Portland cement clinker is a hydraulic material consist of not less than two-thirds by mass of calcium silicates ($(CaO)_3 \cdot SiO_2$ and $(CaO)_2 \cdot SiO_2$), the remainder containing aluminum oxide (Al_2O_3), iron oxide (Fe_2O_3) and other oxides. The ratio by mass $(CaO)/(SiO_2)$ was less than 2.0. The content of magnesium oxide (MgO) did not exceed 5.0 % (m/m). (British Standard Institution BSI 1996).

The strength of the cement in the hydration process from each component, e.g., Tricalcium silicate (C3S) has a medium rate of reaction and heat liberated, Dicalcium silicate (C2S) has a slow rate of reaction and a small heat liberated, Tricalcium alumina (C3A) has a fast rate of reaction large heat liberated, and Tetracalcium aluminferrate (C4AF) has a slow rate of reaction small heat liberated (Edward, 2008). In this study is

the ordinary Portland cement (CEM I 42.5) manufactured by Bamburi Cement Company of Kenya conforming EN 197-1(EN, 2000) was used. It is the most common type of cement in general usage.

3.1.2 Iron powder oxide

Iron powder oxide (Fe_2O_3) is an industrial product resulting from steel production. When used in certain proportions, the iron powder has shown to increase the compressive strength, flexural strength, and splitting tensile strength of concrete (Ghannam et al., 2016). In this study iron powder with a predominant particles size of 200 nm was used as provided. It was used partially as Portland cement replacement at the percentage of 1.5, 2.5, 3.5 and 5% by weight of cement.

Figure 3-1: Iron oxide.

3.1.3 Aggregates

The aggregates used mainly for this study was the natural sand with particles size less than 5 mm, fineness modulus of 2.62, the specific gravity of 2.45 g/cm^3 and water absorption of 5.23%. The crushed stones with a maximum size of 20 mm, specific gravity of 2.76 g/cm^3 and water absorption of 2.58% were used as coarse aggregate. Therefore, the ASTM C33-11 has specific requirements for the aggregates either coarse aggregate or fine aggregate shape as shown in

Table 3-1.

Table 3-1: Grading requirement of fine aggregate

Sieve (specification E11)	Percent passing
9.5 mm (3/8 in)	100
4.75 mm (No. 4)	95 to 100
2.36 mm (No. 8)	80 to 100
1.18 mm (No. 16)	50 to 85
600 µm (No. 30)	25 to 60
300 µm (No. 50)	5 to 30
150 µm (No. 100)	0 to 10
75 µm (No. 200)	0 to 3.0[A,B]

Sources: ASTM C33-11

3.1.4 Water

Water is a part of the concrete, and it gives the liquid characteristic of the fresh concrete. The cement paste saves the amount of water on the surface of the grains of the cement and the grains of the aggregates to complete the hydration reaction of the cement components inside the concrete. Hydration involves many different reactions, often occurring at the same time. As the reactions proceed, the products of the cement hydration process gradually bond together the individual sand and gravel particles and other components of the concrete to form a solid mass (Neville, 2011). In this study water was used for the mixing and the curing of concrete. The water used was tap water from Jomo Kenyatta University of Agriculture and Technology (JKUAT) free from impurities.

3.2 Methodology

Basically, the collecting of information from previous research and literature review available was used to state the usefulness of employing nanoparticles, which have been used in the field of mixing concrete. Also, it provided more information about the using of iron powder oxide in the concrete, e.g., the advantages and the disadvantages of using

this additive as a concrete component and also the potential solutions to mitigate those weaknesses. Moreover, this research has shown the improvement of this materials in the concrete.

3.2.1 Mix proportion

The mix design of the Portland cement concrete grade M25 in this study was done in accordance with BS EN 206-2014 (British Standards Institution, 2014) and BS EN 8500-2-2015(BS 8500-1, 2015). A total of five mixes were prepared in the laboratory. The first mixture denoted M0 was prepared for the control specimen and the mixtures denoted M1 to M4 were prepared with the addition of iron powder. The cement was partially replacement by 1.5, 2.5, 3.5 and 5% by weighing with iron powder. The aggregates used were combined of crushed gravel and fine sand, with the fine percentage of 32% by weighing. The blended cementitious content of all mixtures was 360 kg/m^3. Hand mixing was performed in accordance with BS EN 1881-125-2013 (British Standard Institution, 2013) with a control mechanism to avoid the loss of cementitious materials and water quantified during mixture proportioning.

3.2.1.1 British Standard Method

The concrete design mix is demanding to cover some requirements like workability of fresh concrete, the compressive strength of the concrete at a specific age, and the durability. Therefore, the design process must cover all of these factors that have many effects on the properties of the concrete (building research establishment report 1988).

3.2.1.2 Selecting of the target water to cement ratio

The variability of the strength during the production brought the uncertainty in the selection of the proportions of the materials. The variation appeared in the quality of the used materials, mix proportions due to the production process, and due to sampling and testing. The previous studies have shown that the variation in the concrete due to the three groups as we mentioned can be normally distributed as in Figure 3-2 (building research establishment report, 1988). The chart has two mathematical parameters, the mean (m) and the standard deviation (s). The standard deviation presents the measure of the variation according to equation (3.1).

$$s = \sqrt{\frac{\sum(x-m)^2}{n-1}} \qquad (3.1)$$

Where *x* is an individual result, *n* is the number of results, and *m* is the mean of the n results.

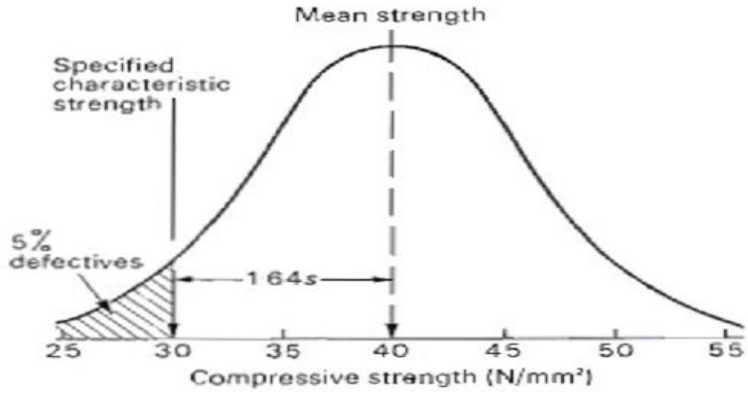

Figure 3-2: Normal distribution of concrete strength.

As the result, the variation leading to design for the mean strength greater than the specific strength, therefore, the differences in the two strengths represented in term of margin M as shown in equation (3.2). In the equation, M = k * s, f_m is the target mean strength, f_c is the specific characteristic strength, s is the standard deviation and k is

constant (10% defectives = 1.82, 5% defectives = 1.64, 2.5% defectives = 1.96, 1.5% efectives = 2.33).

$$f_m = f_c + M \quad (3.2)$$

3.2.1.3 Procedure

The steps of the design can be summarized in the following points:

Step 1: the required strength leading to the w/c ratio.

Step 2: the workability leading to the free water content.

Step 3: step1 and step 2 leading to obtain the cement content.

Step 4: determination of the total aggregate content.

Step 5: the selection of the fine and the coarse aggregate contents.

The assumptions considered for the determination of the mix proportions were: characteristic compressive strength is 25 N/mm^2 at 28 days with 2.5% defectives, slump required was 30 to 60 mm, nominal maximum aggregate 20 mm (uncrushed), fine aggregate 60% passing 600 µm sieve (uncrushed), water-free / cement ratio 0.5 and minimum cement content 300 kg.

The target mean strength of Figure 3-2 is used to determine the w/c ratio. Table 3-2 gives the strength depending on 0.5 w/c ratio, and type of the cement and the aggregate. This strength should be plotted in appendix 3 and obtain the exact w/c ratio.

Table 3-2: Compressive strength of concrete mixes made with a free water/cement ratio of 0.5

Type of cement	Type of coarse aggregate	Age (days)			
		3	7	28	91
		Compressive strength (N/mm^2)			
Ordinary Portland or	Uncrushed	22	30	42	49

Sulphate resistance Portland	Crushed	27	36	49	56
Rapid hardening Portland	Uncrushed	29	37	48	54
	Crushed	34	43	55	61

The same approach has been used to obtain the free water contents in kilogram per unit volume to give different values for workability as in Table 3-3.

Table 3-3: Free-water content required to give various levels of workability

Slump (mm)		0 – 10	10 – 30	30 – 60	60 – 180
Vibe time (s)		> 12	6 – 12	3 – 6	0 – 3
Maximum size aggregate (mm)	Type of aggregate	Water content (kg/m^3)			
10	Uncrushed	150	180	205	225
	Crushed	180	205	230	250
20	Uncrushed	135	160	180	195
	Crushed	170	190	210	225
40	Uncrushed	115	140	160	175
	Crushed	155	175	190	205

Therefore, the determination of the total aggregate contents will follow the above step by using the figure in the Appendix 3, the fine aggregate and the coarse aggregate will obtain from these charts and combines the proportions of the total aggregate and the proportion of the fine aggregate to obtain the coarse aggregate (building research establishment report, 1988).

3.2.2 Preparation of test sample

All the mixtures were produced by blending the fine aggregates, coarse aggregates and cementitious materials (cement and iron powder) in the laboratory using hand mixing. They were mixed in a dry condition before adding fresh water. For the control mixture, only cement was used. slump test and compaction factor test of the fresh concrete were performed promptly to evaluate the consistency of the mixture in accordance with the mixing procedure (Figure 3-3). The concrete was poured in three different types of mold,

cubes of 100 mm and 150 mm sides with a cylinder of 100 mm diameter and 200 mm long. The test specimen were stored in moist air for 24 hours after casting. After this period the specimen were demoulded, marked and cured in clear fresh water until taken out to test. The compressive and tensile strengths tests were performed on the concrete samples at 7, 14 and 28 days. The porosity of the hardened concrete was also determined. The results shown are the mean of three samples test.

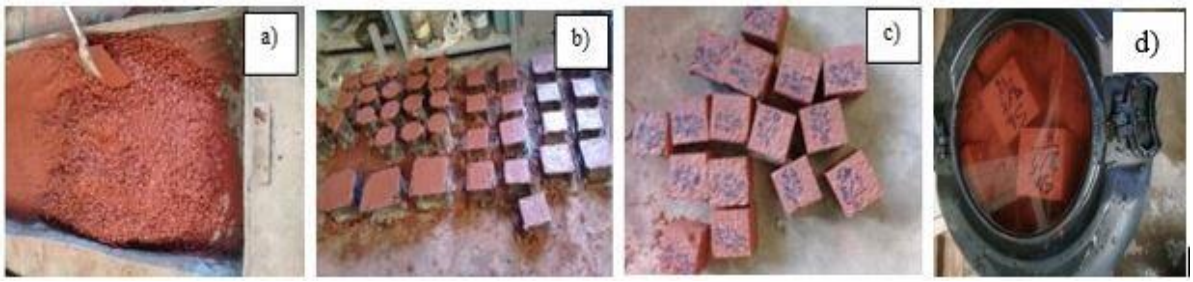

Figure 3-3: Preparation of samples.
In the figure; a) mixing; b) casting; c) demolding; d) curing

3.2.3 Material characteristic tests

Tests will be done to determine the properties of the constituent materials. Samples of NCA, Iron powder; Cement, and Sand will all be taken to the laboratory to test for water absorption, density, specific gravity, particle size distribution, fineness, and chemical composition.

3.2.4 Physical properties of materials

3.2.4.1 Cement and iron powder

The chemical composition of the binder (cement and iron powder) have been determined at the laboratory of the ministry of mining of Kenya. The physical properties of the iron

powder have been given by the supplier. The specific gravity and bulk density of cement have been determined in the laboratory of the civil engineering department of JKUAT.

3.2.4.2 Aggregates

Parameters like particle size distribution, bulk density, specific gravities, water absorption, and voids content of fine and coarse aggregates were of great importance and were tested in accordance to the standard methods summarized in Table 3-4. The voids content of the fine and coarse aggregate can be computed according to ASTM C29 as presented in equation (3.3). In the equation, M is the bulk density of aggregate (kg/m^3), S is bulk specific gravity as determined in accordance with test method C127 or test method C128, and ρ_w is the density of water.

$$Voids\ (\%) = \ (S \times \rho_w - M)/(S \times \rho_w\ ) \quad (3.3)$$

Table 3-4: Recapitulation of the standard used

Designation	Methods	
	Fine aggregates	Coarse aggregates
Specific gravity Apparent Specific gravity Water Absorption	ASTM-C128 (AASHTO T84)	ASTM-C127 (AASHTO T85)
Voids content	ASTM C29	ASTM C29
Particles size distribution	ASTM C136/ASTM C33/11	ASTM C136/ASTM C33/11

3.2.5 Fresh properties of concrete

The slump test and compactor factor of the mixtures were conducted in conformance with the test method as specified in BSI 1881-102 (1983) and BS 1881-103 (1983) (British Standards Institution, 1983) in order to determine the workability of the concrete. The fresh density of concrete was also determined. Figure 3-4 shows the slump

measurement and compaction factor test.

Figure 3-4: Slump measurement (a) and compaction factor test (b).

3.2.6 Mechanical properties tests

3.2.6.1 Compressive strength test

The cubes specimen of 100 mm x 100 mm x 100 mm of dimensions were casted to determine compressive strength. A total of 33 cubes were casted and cured at 7, 14, 28 days of moisture curing condition in accordance with the prescribed methods BSI 1881-115 (1983) (British Standard Institution 1881). The test equipment used was the universal testing machine (UTM) and the compressive strength was performed at 7, 14, and 28 days. Figure 3-5 shows the compressive strength test.


Figure 3-5: Compressive strength test.

3.2.6.2 Tensile splitting strength test

The tensile strength test (Figure 3-6) was conducted on the cylinder of 100 mm diameter and 200 mm height in accordance with the standard test method BSI 1881-117-1983(British Standards Institutions, 1983). The samples were tested after 7, 14, and 28 days of curing.

Figure 3-6: Tensile splitting test.

3.2.6.3 Water absorption, density and porosity tests

Water absorption densities and permeable porosity in concrete were determined using equations (3.4) to (3.10) in accordance with the standard test method ASTM C642-2013 (ASTM C642-13, 2013). A total of 30 samples of cubes 100 mm x 100 mm x 100 mm of dimensions were casted and cured for 28 days in water. The specimen were dried in an oven until the difference of two successive values of mass was less than 0.5% of the lesser value. After drying and cooling, the samples were immersed in water at a temperature of 21˚C for 72 hours to determine the saturated mass after immersion. The specimen were placed in a receptacle, covered with tap water and boil for 5 hours. They were cooled by natural loss of heat for 15 hours to a final average temperature of 22.5 ˚C and the saturated mass after immersion and boiling were determined. In final, the

specimen were suspended by a wire in water after immersion and boiling, then the apparent mass in water was determined. The result reported was the average of three samples of concrete.

$$\text{Absorption after immerson } (\%) = [(B - A)/A] \times 100 \quad (3.4)$$

$$\text{Absorption after immersion and boiling } (\%) = [(C - A)/A] \times 100 \quad (1.5)$$

$$\text{Permeable porosity }, \% = [(C - A)/(C - D)] \times 100 \quad (3.6)$$

$$\text{Bulk density, dry} = [A/(C - D)] \times \rho = g_1 \quad (3.7)$$

$$\text{Bulk density after immersion} = [B/(C - D)] \times \rho \quad (3.8)$$

$$\text{Bulk density after immersion and boiling} = [C/(C - D)] \times \rho \quad (3.9)$$

$$\text{Apparent density} = [A/(A - D)] \times \rho = g_2 \quad (3.10)$$

In the equations, A is mass of oven-dried sample in air (g), B is mass of surface-dry sample in the air after immersion (g), C is mass of surface-dry sample in the air after immersion and boiling (g), D is apparent mass of sample in water after immersion & boiling (g), g_1 is dry bulk density (Mg/m^3), g_2 is apparent density (Mg/m^3) and ρ is density of water (g/cm^3).

3.2.6.4 Sorptivity

The rate of absorption of water/liquids (sorptivity) is an easily measured material property which characterizes the tendency of a porous material to absorb and transmit water by capillarity. Its theoretical basis in unsaturated flow theory is reviewed, together with methods of measurement suitable for cement-based materials(Hall, 1989). In unsaturated concrete, the rate of ingress of water or liquids is largely controlled by absorption due to capillary rise. The water absorption of a concrete surface depends on many factors including: concrete mixtures proportions; the presence of chemical

admixtures and supplementary cementitious materials; the composition and physical characteristic of cementitious component and of the aggregates; the entrained air content; the type and duration of curing; the degree of hydration or age; the presence of microcracks; and the presence of surface treatment such as sealers or form oil. In this study, the sorptivity was determined according to the standard test method ASTM C1585 (2013) (ASTM C1585 - 2013). Cubes samples of 150 mm x 150 mm x 150 mm of dimensions were casted and cured for 28 days before taking for the test. A total of 15 specimen were prepared to measure the rate of absorption. The specimen were conditioned inside an oven at a temperature of 50 ±2˚C for 3 days. After 3 days, the specimen were each placed inside a sealed container and stored at 23 ±2˚C for 15 days before the absorption procedure started (Figure 3-7).

The specimen were removed from the storage container, their mass recorded before the sides surface sealed. The side surface of the specimen that will not be exposed to water was sealed with epoxy (Figure 3-8). The mass of the sealed specimen was recorded for each sample and set as initial mass for water absorption calculations. The mass of each specimen in contact with water was recorded at the intervals shown in Table 3-5. The absorption, I (equation 3.11) is the change in mass divided by the product of the cross-sectional area of the test specimen and the density of water. For the purpose of this test, the temperature dependency of the density of water is neglected and a value of 0.001g/mm^3 is used. Figure 3-7 and 3-8 show the specimen inside the container and the schematic of the procedure. In the equation, I is the absorption (mm), m_t is the change in specimen mass (g), at the time t, a is the exposed area of the specimen (mm^2) and d the density of water (g/mm^3).

$$I = \frac{m_t}{a \times d} \tag{3.11}$$

Figure 3-7: Specimen inside a sealed container.

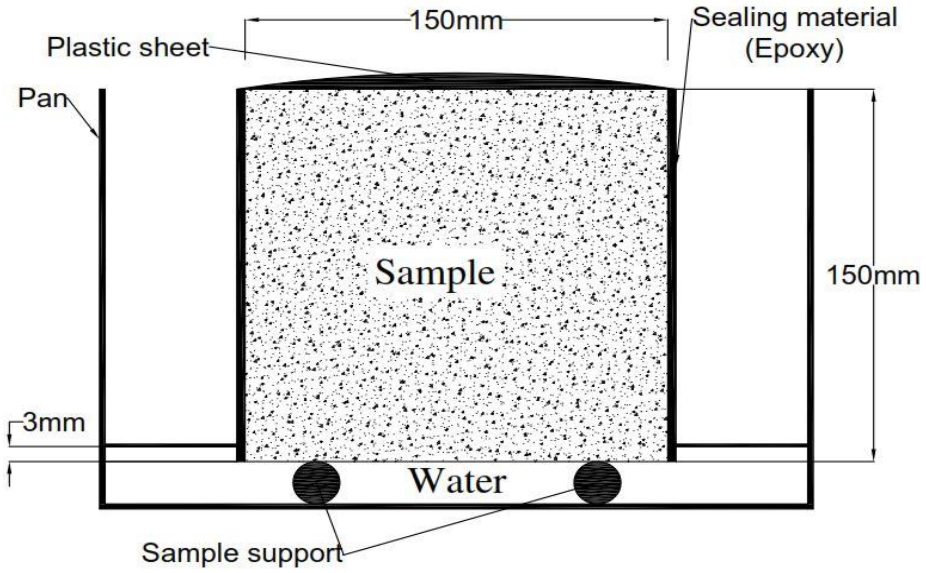

Figure 3-8: Schematic of the procedure.

Table 3-5: Times and tolerances for the measurements schedule

Times									
Minutes									
1	5	10	20	30	60	Hourly up to 6 h	Once a day up to 3 days	Day 4 to 7 3 measurements 24 h apart	Day 7 to 9 1 (one) measurement
Tolerances									
Seconds		Minutes					Hours		
2	10	2	2	2	2	5	2	2	2

3.2.7 Durability performance

a) Chloride penetration test of concrete

Reinforced concrete structures are exposed to harsh environments yet are often expected to last with little or no repair or maintenance for long periods of time (often 100 years or more). To do this, a durable structure needs to be produced. For reinforced concrete bridges, one of the major forms of environmental attack is chloride ingress, which leads to corrosion of the reinforcing steel and a subsequent reduction in the strength, serviceability, and aesthetics of the structure (Stanish et al., 1997). This may conduct to the early maintenance or premature replacement of the structure.

The objective of this test was to assess the capability of the iron powder concrete to resist chloride penetration. The test was performed on cylinders specimen of the diameter of 100 mm and the height of 200 mm of the casted concrete mixture. The test was calibrated to be performed at different ages of the concrete specimen, at 30, 45 and 60 days. For that purpose, after 28 days curing period was over, the specimen were submerged into a sodium chloride solution at 3% for a duration of 30, 45 and 60 days. Chloride penetration was obtained by using a colorimetric method by applying nitrate silver ($AgNO_3$) solution upon split concrete specimen (Javier et al., 2017). The presence of this solution on the concrete specimen caused reactions and a change of color. The depth of penetration is generally in white color and the yellow color represent the region that there were no signs of chloride attack.

b) Acid attacks

Acid attacks were conducted on cubes 100 mm x 100 mm x 100 mm of dimensions to study the effect of water containing hydrochloric acid at various percentage (2% and 3%)

on concrete. A total of 90 samples were prepared for the purpose. Prior to exposing the samples to the solution, they were cured for 28 days in water. Our target here was to assess the weight loss of cubes specimen and the compressive strength loss at the specific ages of 30, 45 and 60 days. The results reported were the average of three values.

3.2.8 Structural performance of reinforced and non-reinforced concrete beam

a) Experimental work

Twelve concrete beams were casted, of which six reinforced concrete beams with the dimensions of 150 mm wide by 150 mm depth by 1000 mm long as shown in Figure 3-9 and six others none reinforced concrete beams with the dimensions 150 mm wide by 150 mm depth by 550 mm long (Figure 3-10) were prepared for an anticipated flexural failure. Among the six reinforced concrete beams, three were made without iron powder and taken as control specimen, and three others were made with 2.5% iron powder. The none-reinforced concrete beams were also made the same as shown in Table 3-6. The concrete beams were reinforced using two 10 mm diameter rib bars (Y10), two 8 mm rid bars (Y8) and 6 mm links (R6) at space of 150 mm. The measured yield and ultimate strengths of the Y10 rib bars were 611.465 N/mm^2 and 680.25 N/mm^2, while those of the Y8 plain bars were 537.42 N/mm^2 and 673.028 N/mm^2. All the concrete beams were cast using the same batch of the concrete mix, cured in the same regime and had the same thickness of concrete cover of 25 mm.

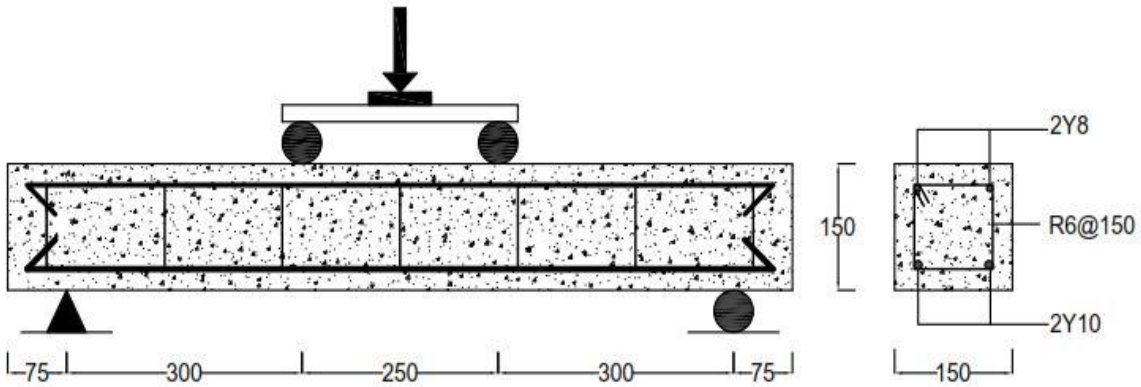

Figure 3-9: Specimen of the reinforced concrete beam.

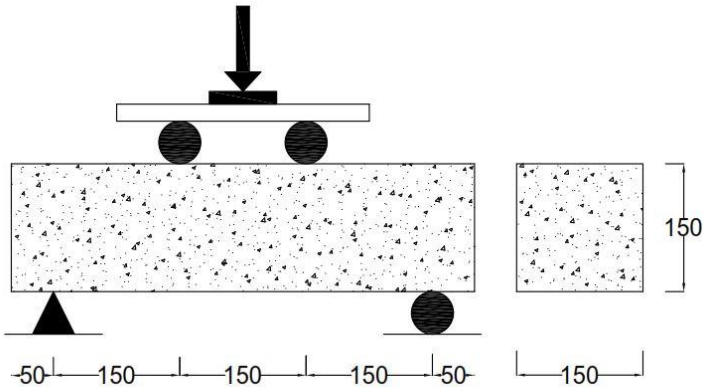

Figure 3-10: Specimen of the none-reinforced concrete beam (NRC-B)

Table 3-6: Beams type with dimensions

Type of beam	Control: concrete without iron powder		Concrete with 2.5% iron powder	
	Nber	Dimensions (mm)	Nber	Dimensions (mm)
None-reinforced concrete beam	3	150 x 150 x 550	3	150 x 150 x 550
Reinforced concrete beam	3	150 x 150 x 1000	3	150x 150 x 1000

For the purpose of the investigation of structural performance on the different beams, a set of equipment and materials was used for specific needs: a load cell, which is an electronic device (Transducer), was used for recording of loadings applied, the electrical device for precision measurement of displacements named LVDT (Linear Variable Displacement Transducer) was placed at the middle of beams for measuring deflections,

electrical strain gauges of concrete of 60 mm length were used for measuring flexural strain on the concrete and the data logger or strain meter used to read, translate and record the outputs data.

b) Four points flexural test

None-Reinforced concrete beam: Two sets of 3 beams were tested under four points bending test. The first set was made up of concrete specimen without iron powder taken as control denoted NRC-B0, and the second set with 2.5% iron powder replacement in the concrete, denoted NRC-B1. Each beam was water cured for 28 days before testing. The tests were carried out by placing the beams on the universal testing machine (UTM) as shown in Figure 3-11. The main parameters of interest recorded for analysis were: the ultimate load and the maximum strength, the mode of failure and crack patterns and the concrete stress-strain characteristics (tensile)

Reinforced concrete beam: Two types of beams were tested under four points bending test. The first set was made up of reinforced concrete specimen without iron powder taken as control denoted RC-B0, and the second types with 2.5% iron powder content in the concrete matrix, denoted RC-B1. Each beam was water cured for 28 days before testing. The tests were carried out by placing the beams on two supporting pins, set at a particular distance apart as shown in Figure 3-12.

Each beam was instrumented with one concrete strain gauge, an LVDT and a load cell, all connected to a data logger. The tensile strain of beam specimen was measured through concrete strain gauge placed longitudinally at the bottom along the axis of the beam. The data logger was then recording all the specific data transmitted by those censors during the test until failure. The main parameters of interest recorded for analysis, were: the first

crack and ultimate load, the mid-span deflection, the mode of failure and crack patterns, and the concrete stress-strain characteristics (tensile and compressive).

Figure 3-11: Set up of four points bending test on UTM.

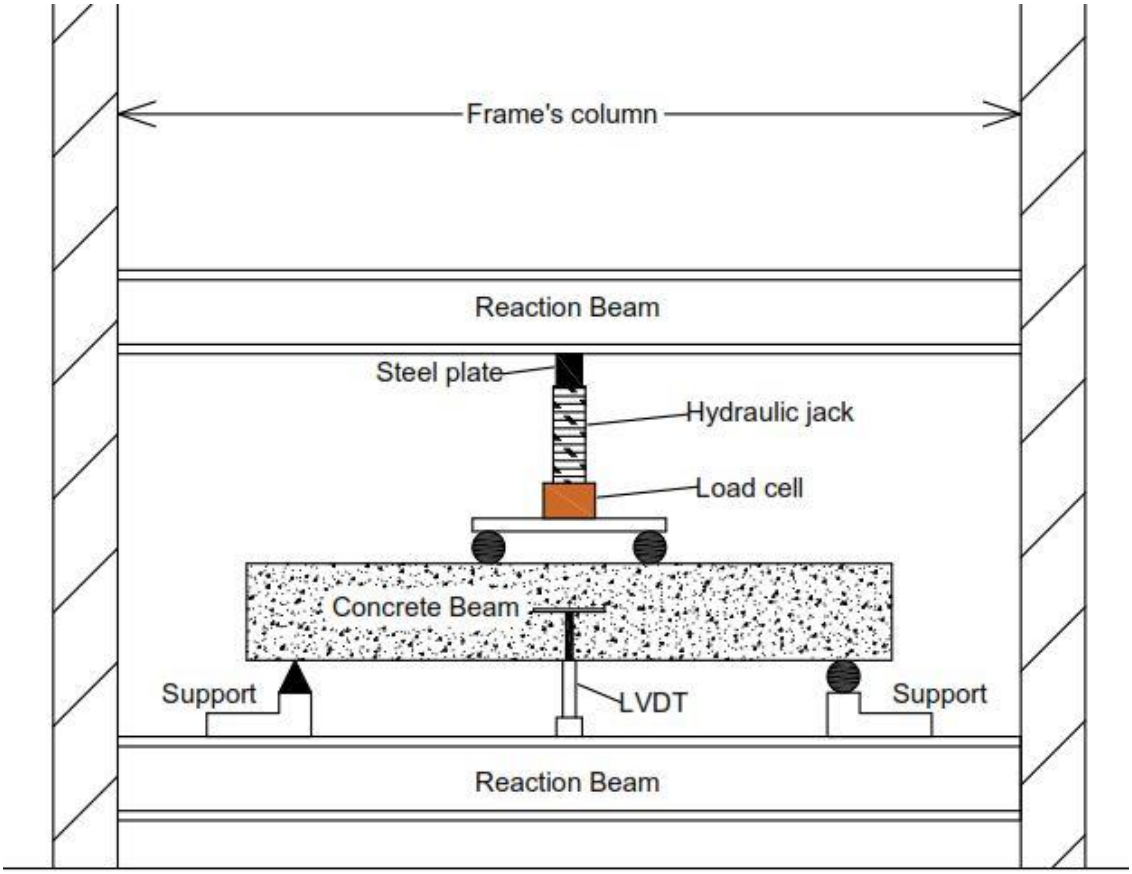

Figure 3-12: Test rig for four points bending.

CHAPTER FOUR

4 RESULTS AND DISCUSSION

4.1 Physical Properties of Materials

4.1.1 Cement and Iron powder

The ordinary Portland cement type I (CEM 42.5) supplied by Bamburi Cement Ltd Company was used for this study. Iron powder (Fe2O3) with a predominant particles size of 200 nm was used as provided. Table 4-1 gives the result of the physical properties of cement carried out at the Structural and Materials Laboratory of Jomo Kenyatta University of Agriculture and Technology and

Table 4-2 the technical data of iron powder. The chemical composition was carried out at the laboratory of the ministry of petroleum and mining of Kenya.

Table 4-3 gives the chemical composition of the cement and iron powder used for the experiment.

Table 4-1: Physical properties of Portland cement

Specific gravity	Loose bulk density (kg/m3)	Compacted bulk density (kg/m3)
3.185	1162.3	1398

Table 4-2: Physical properties of the iron powder from china

TECHNICAL DATA Designation	Min	Max	Test Method
Water-Soluble Content [%]		1	ASTM D 1208
Oil Absorption [g/100g]	15	25	ASTM D 281
Sieve Residue（0.045mm）[%]		0.5	ASTM D 185
Predominant Particle size [μM]	0.2		Electron Micrographs
Fe2O3 [%]	95		ASTM D 50
SiO2+Al2O3 Content [%]		0.6	DIN 55913
Moisture (After Production) [%]		1	ASTM D 280
Loss on Heating 1000℃1/2h [%]		5	ASTM D 1208
Particle Shape	Spherical		Electron Micrographs

Density [g/ml]	∼5.0	ASTM D 153

Table 4-3: Chemical composition of cement and iron powder

Parameters	Cement	Iron powder
SiO2	20.62	4.21
Al2O3	5.04	2.67
Fe2O3	3.23	88.31
CaO	63.36	0.36
MgO	0.82	2.22
SO3	2.73	
Na2O	0.16	0.04
K2O	0.53	0.02
TiO2	-	0.01
MnO	-	0.21
Free CaO	0.63	-
Na Eq	0.48	-
Cl-	< 0.01	-
LOI	2.9	1.01
I.R	1	-
C3A	7.91	-

Table 4-3 is giving the result of the chemical composition of the Portland cement. It can been seen that the calcium silicate is almost 84% of the mass. This value must be two-thirds by mass and the content of magnesium oxide shouldn't exceed 5% (BSI 1996). Here the result gives 0.82 % of magnesium oxide. The iron oxide is pure at 88% content by mass.

4.1.2 Physical properties of aggregates

a) Particles size distribution

The particle size distribution test was performed according to ASTM C136. Oven dried sample of 1000g of ordinary sand was taken to perform sieve analysis. The grading result of fine and coarse aggregate found are displayed in Figure 4-1 and Figure 4-2

respectively. As it showed in the figures, the passing percentage met the grading requirement limitations of ASTM C33/C33M-(2011).

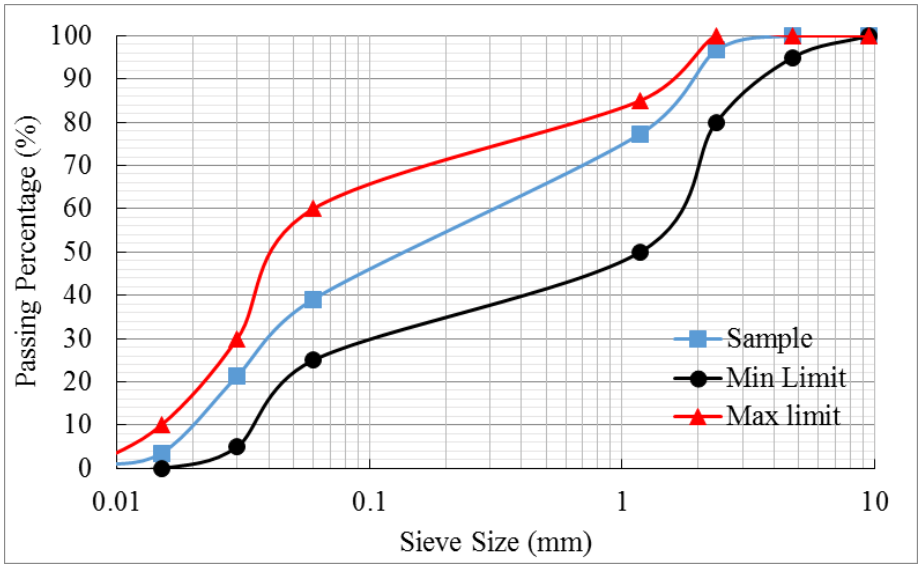

Figure 4-1: Particles size distribution of fine aggregate.

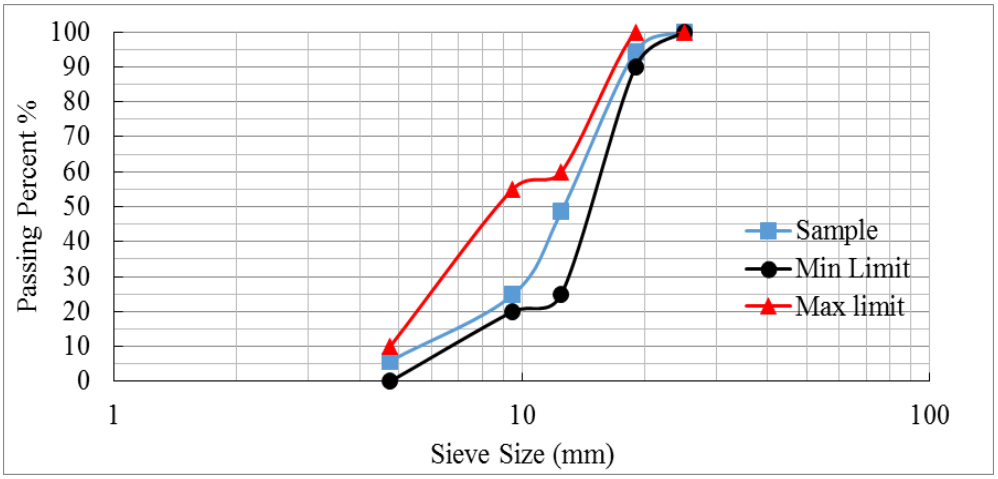

Figure 4-2: Particles size distribution of coarse aggregate.

Fineness modulus obtained was 2.62 and was within the acceptable range. It was computed as sum of cumulative percent from sieve 9.5 to 0.015mm divided by 100. According to the standard ASTM C33/33M (2011), fineness modulus shall be within 2.3 to 3.1.

b) Specific gravity and water absorption of aggregates

The specific gravity and water absorption of fine aggregate were carried out in accordance with ASTM-C128 (AASHTO T84), for the coarse aggregate as prescribed in the standard ASTM-C127 (AASHTO T85). Samples of 0.5 Kg of fine and 3 kg of coarse aggregate was taken to perform the test, the result is given as shown in table 4-4.

Table 4-4: Specific gravity and water absorption of fine and coarse aggregates

Designation	Fine aggregates	Coarse aggregates
Specific gravity	2.45	2.76
Apparent Specific gravity	2.65	2.89
Water Absorption	5.23	2.58

c) Bulk density and voids content of loose and compacted aggregates

The voids content of the fine and coarse aggregate can be computed according to ASTM C29 as in equation (4.1). In the equation, M is the bulk density of aggregate (kg/m^3), S is bulk specific gravity as determined in accordance with test method C127 or test method C128, and ρ_w is the density of water. The results of the voids content are given in the Table 4-5.

$$\text{Voids } (\%) = (S \times \rho_w - M)/(S \times \rho_w) \quad (4.1)$$

Table 4-5: Void content of loose and rodded aggregates

Designation	Fine aggregate		Coarse aggregate	
	Loose	Rodded	Loose	Rodded
Bulk density (kg/m^3)	1420	1607	1335	1470
Void content (%)	41.83	34.19	51.46	46.56

4.1.3 Mix design proportions

The method of mix design applied in this study was the method prescribed by BS 5238-1981(see Appendix 1). The design was carried out using the procedure of this standard and the result is presented in Table 4-6.

Table 4-6: Details of mix design proportions

Designation	Iron powder content (%)	Quantities (kg/m^3)					
		Cement	Water	Fines	Coarse	W/C	Nano-Fe_2O_3
M0	0	360	180	585.6	1244.4	0.500	0
M1	1.5	354.6	180	585.6	1244.4	0.508	5.4
M2	2.5	351	180	585.6	1244.4	0.513	9
M3	3.5	347.4	180	585.6	1244.4	0.518	12.6
M4	5	342	180	585.6	1244.4	0.526	18

4.2 Workability Fresh Concrete

The strength and durability of concrete in its lifetime is relatively dependent on his degree of its workability. Workability is the ability of a fresh concrete mix to fill the form/mold properly with the desired vibration and without reducing the concrete's quality. Workability depends on water content, aggregates, cementitious content and can be modified by adding chemical admixtures, like superplasticizer. Raising the water content or adding chemical admixtures increases concrete workability. Fresh concrete test concerned slump test and compaction factor test. These tests carried out to determine the workability and consistency of each mix.

Slump test conducted in accordance with the standard prescribed in BS 1881-102 (1983) in order to determine the consistency of the different concrete mix. For the concrete mix design considered, the specified slump was from 25 – 75 mm. As a procedure, “Abrams cone” was filled in three layers, each layer compacted 25 times using a tamping rod with a diameter of 16 mm. The compaction factor test conducted as specified by the standard BS 1881-103 (1983) performed in order to determine the workability of the different concrete mixes.

The maximum strength of concrete is related to the workability and can only be obtained if the concrete has an adequate degree of workability because of self-compacting ability (Nazari et al., 2010). From Figure 4-3, the results showed that when iron red powder was added as partial replacement of cement, the slump starts decreasing. It is showing also that there is a strong correlation between the quantity of iron red oxide and the workability of concrete mixes (R^2 = 0.9439). The slump of the control sample was 40 mm, which consequently decreases to 16 mm when about 5% of cement replaced by iron red oxide. From regression analysis, equation (4.2) was found from a linear form relationship. In the equation, S is the slump (mm) and P is the percentage content of iron powder.

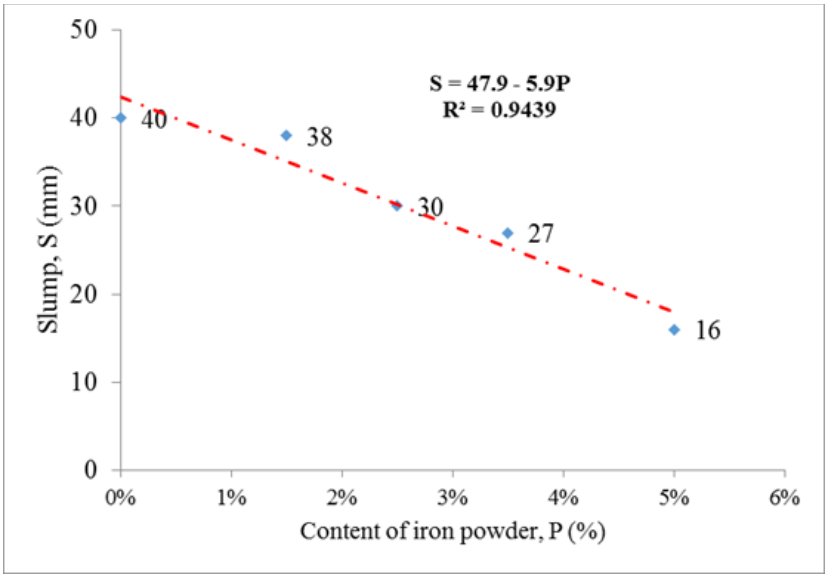

Figure 4-3: Slump variation for different mixtures with iron red powder.

$$S = 47.9 - 5.9P \quad (4.2)$$

From Table 4-7, the value of the compaction factor varies from 0.97 to 0.89. The result showed that the compaction factor decreased when the iron powder is added. The regression analysis was run to define the relationship between the slump and compaction

factor (Figure 4-4), it was found that there is a strong correlation between them as the coefficient of determination R^2 is 0.9709.

Table 4-7: Fresh properties of different concrete mixtures

Fresh properties	Concrete mixtures (%)				
	M0	M1	M2	M3	M4
	0.0	1.5	2.5	3.5	5.0
Slump (mm)	40	38	30	27	16
Compaction factor	0.97	0.95	0.93	0.91	0.89
Fresh density (g/cm^3)	2311	2297	2378	2340	2380

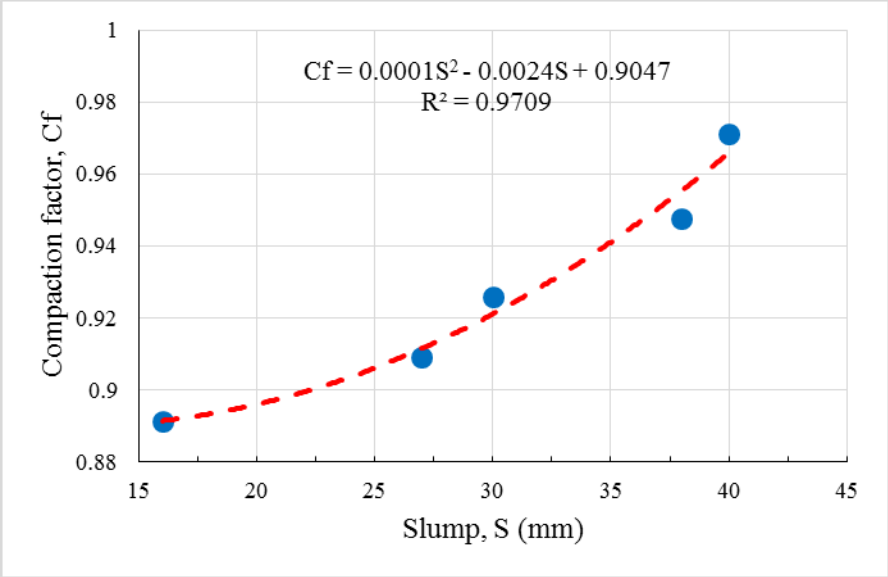

Figure 4-4: Relation between compaction factor and slump test

This result can be justified by the fineness of iron powder (0.2µm) and its high water absorption. However, almost all the mixes felt in the expected range of a slump (between 25-75mm) except when 5% of iron powder was added and the compaction factor felt with the ranges specified by the standard BS 1881-103(1983).

4.3 Hardened Concrete Test

4.3.1 Compressive strength

The results for the compressive strength of iron powder blended Portland cement obtained at seven, fourteen, and 28 days and their standard deviation are shown in Figure 4-5. The results showed that when 1.5 and 2.5% of cement replaced by iron-red powder the compressive strength increased by 11.17 and 27.03% at 28 days, respectively. The introduction of iron powder at the levels of 3.5 and 5% show decreasing of compressive strength by 7.14, 16.68% at 28 days respectively. The experiment results from the previous research showed that the use of nano-Fe_2O_3 particles up to a maximum replacement level of 2.0% produces concrete with improved strength. However, the ultimate strength of concrete was gained at 1.0% of cement replacement(Dai et al., 2000). In this study, the highest improvement of compressive strength was gained at 2.5% iron powder content, at 28 days the strength reached 33.64 MPa for a concrete grade of M25.

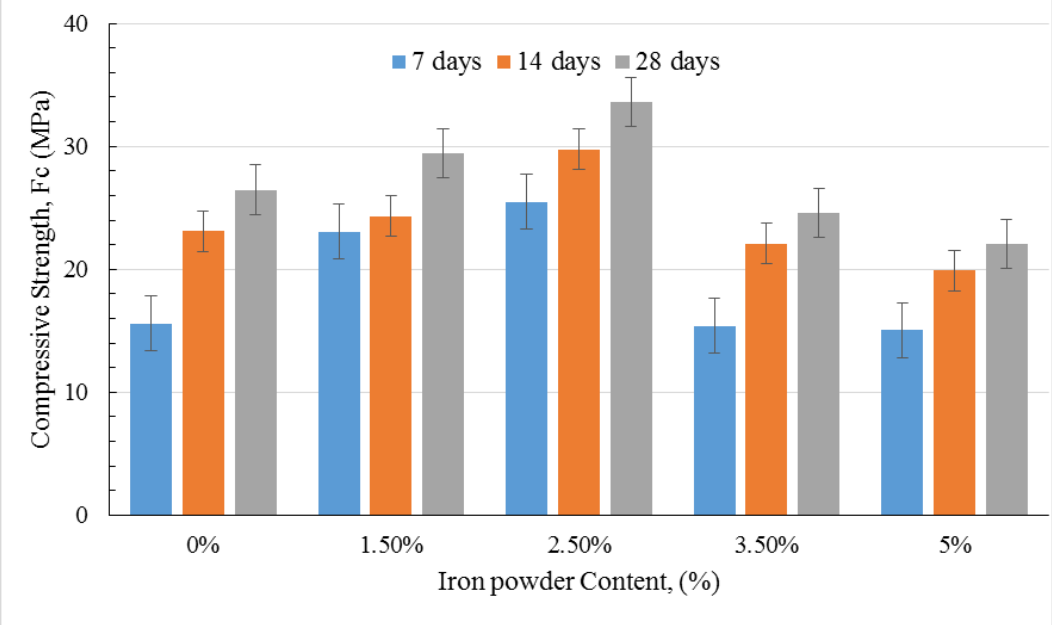

Figure 4-5: Compressive strength at 7, 14, and 28 days versus content of iron powder.

This phenomenon can be explained as when the iron powders are uniformly distributed in concrete each particle has a cubic pattern and distance between the nanoparticles is adjustable (Branch et al., 2011). The particles due to their micro fine size, they fill the pores (the nano-filler effect), leading to the further compacting of the microstructure. These main phenomena lead to the improvement of the microstructure by reducing the amount of pores, improving the bond between the aggregate and the cement matrix and increasing the density of the cementitious composite (Sikora et al., 2016). The high improvement of compressive strength in the blended concrete is due to the rapid consumption of $Ca(OH)_2$ which was formed during hydration of Portland cement especially at early ages related to the high reactivity of nano- Fe_2O_3 particles (Dai et al., 2000).

4.3.2 Tensile splitting strength

The results obtained from tensile splitting strength test at 7, 14, and 28 days are depicted in Figure 4-6. The experiment showed that when 1.5% of cement replaced by iron-red powder, the split tensile strength increased by 4.63% at 28 days. It showed also that when the replacement level at 2.5, 3.5 and 5%, the tensile strength decreased by 3.24, 6.48 and 13.43%, respectively, at 28 days. From previous research, results showed from the sample containing 1 and 3% Fe_2O_3 nanoparticles, the mechanical properties have improved than the ordinary cement mortar. The results show that the addition of Fe_2O_3 Nanoparticles, increasing amount of compressive strength is more than tensile strength (Branch et al., 2011).

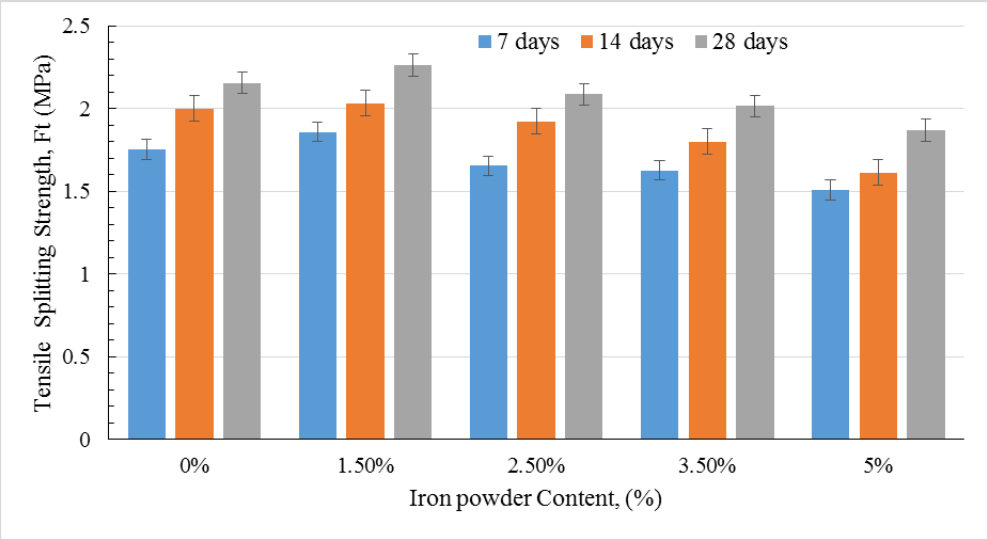

Figure 4-6: Tensile splitting strength at 7, 14, and 28 days versus iron powder content.

It was also observed from the previous study, that 1.0% replacement caused a decrease in the split tensile strength of the experimental cement (Arefi et al., 2012). In this study, split tensile strength started decreasing when the replacement higher than 1.5% (2.5 to 5%). This may be due to the fact that the quantity of Fe_2O_3 particles present in the mixture was higher than the amount required to combine with the liberated lime during the hydration process, thus leading to excess silica leaching out and causing a deficiency in strength as it replaced a part of the cementing material but did not contribute to its strength (Nazari et al., 2010).

4.3.3 The relationship between iron powder, tensile and compressive strength

The compression and tensile strengths of hardened concrete at 28 days versus the iron powder amounts are shown in Figure 4-7 and Figure 4-8. It is easily observed on the polynomial growth tendency of the compressive and tensile strength when cement was partially replaced by iron powder, there was an improvement in strengths. For example, the compressive strength of the control sample at 28 days was 26.48 MPa, which

gradually improved to about 33.64 MPa when 2.5% of iron powder is added. Subsequently, this value slowly decreases to about 22.06 MPa when 5% of iron oxide is incorporated. Hence, there should be a maximum amount of iron red oxide, where the compressive and tensile strengths can be theoretically the largest.

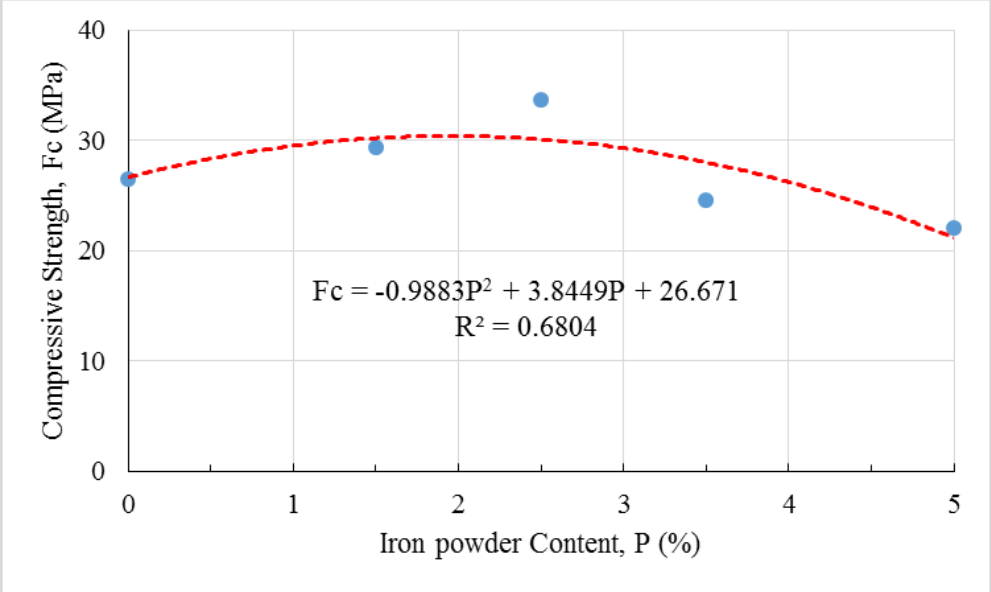

Figure 4-7: Relation between iron powder content and compressive strength at 28 days.

From the regression analysis equations (4.3) and (4.4) were found, it is easy to interpret that when the differential coefficient (y') of each function equals to zero, the value of P represents the optimal amount of iron red oxide to obtain the best mechanical properties. The differential coefficient (y') are found from the derivation of equation (11) and (12). In the equations, F_c is the compressive strength (MPa), F_t is split tensile strength (MPa) and P the amount of iron powder in percentage (%).Therefore, the optimal amount of iron red powder and the calculated maximum compressive and tensile strengths at 28 days are shown in Table 4-9.

$$F_c = -0.9883 \times P^2 + 3.8449 \times P + 26.671 \quad (4.3)$$

$$F_t = -0.0183 \times P^2 + 0.0248 \times P + 2.1831 \quad (4.42)$$

Table 4-8: Optimal amount of iron oxide for compressive and tensile strengths at 28 days

Values	Compressive	Tensile
Optimal iron oxide (%)	1.95	0.68
Computed maximum strength (MPa)	30.41	2.19
Coefficient of determination (R^2)	0.68	0.88

As it can be seen, the optimal amount of iron powder for compressive and split tensile strength at 28 days are 1.95 and 0.68%, respectively. The corresponding compressive and tensile strengths are 30.39 and 2.19 MPa, respectively. The computed compressive strength at 28 days is smaller than the experimented one with 2.5% of iron powder (33.64 MPa). This can be interpreted with the deviation of the regression analysis equation. From a regression analysis, a polynomial form relation was found between compressive strength and split tensile strength at 28 days as displayed in equation (4.5) and Figure 4-9. The coefficient of determination $R^2 = 0.9505$. In the equation, F_c and F_t are compressive strength and split tensile strength respectively, in MPa.

$$F_t = -0.007 \times {F_c}^2 + 0.4103 \times F_c - 3.8143 \quad (4.5)$$

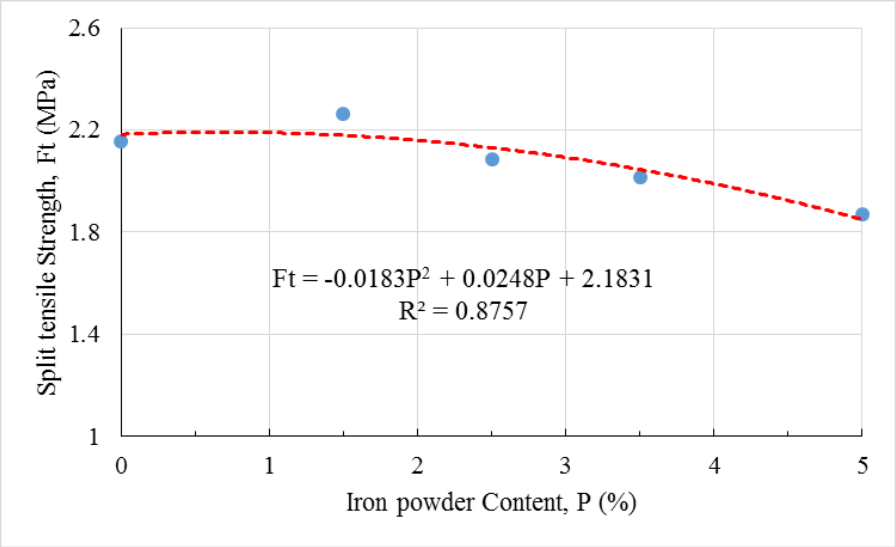

Figure 4-8: Relationship between Iron powder content and tensile splitting strength at 28 days.

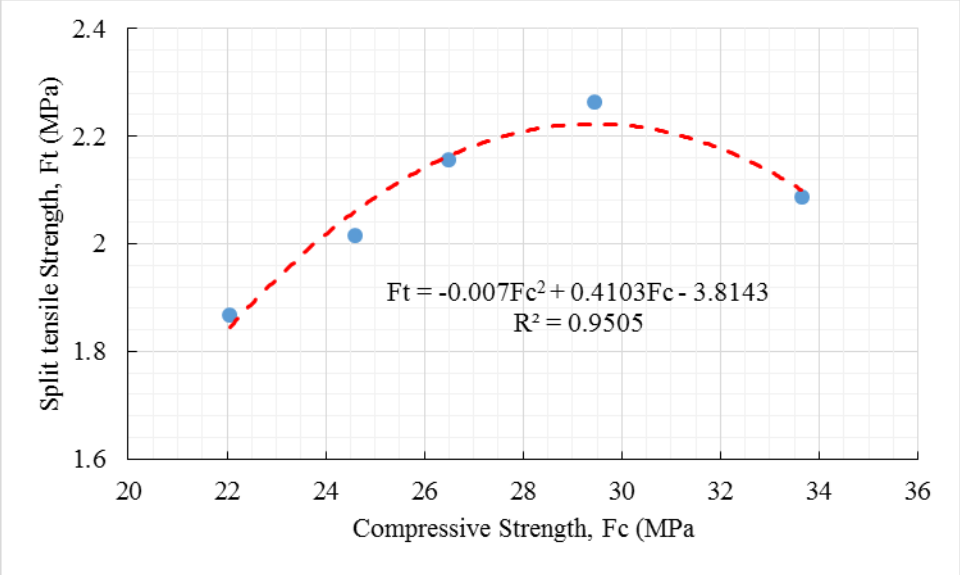

Figure 4-9: Relationship between compressive and tensile strength at 28 days.

4.3.4 Water absorption

Two different types of water absorption were determined using the standard test methods ASTM C-642-97, Water absorption after immersion (Wai), and water absorption after immersion and boiling (Waib). The result obtained in Figure 4-10, showed that Wai, and Waib decreased up to 20.8 and 20.92%, respectively, when 2.5% of Portland cement is

replaced by iron powder. Wai and Waib started increasing respectively up to 8.02% and 8.28% when 5% of the content of iron powder added. The values of Wai are somewhat higher than Waib values. In the mixtures where 0.5 and 1.25% nano-Fe_2O_3 was added, capillarity dropped by 5 and 1%, respectively. On the other hand, the addition of this powder at a proportion of 2.5% increased the capillarity by 3%. Indeed as indicated in the previous study (Oltulu & Şahin, 2013). In this study, the water absorption decreased up to a minimum value of 2.5% of replacement and increased to a maximum value of 5% of cement replacement. The water absorption was correlated to iron powder content in a polynomial function as shown in equations (4.6) and (4.7). In the equations Wai is water absorption after immersion (%), Waib, water absorption after immersion and boiling (%), and P the iron powder content in percentage (%).

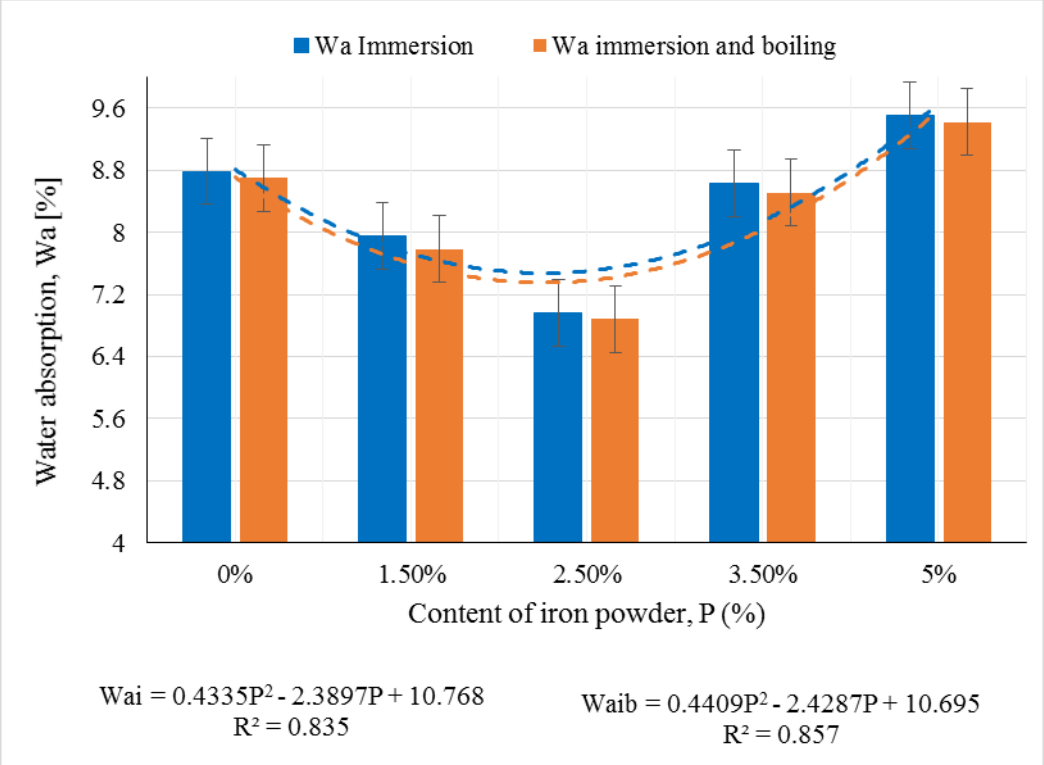

Figure 4-10: Wai & Waib variation versus the content of iron red powder.

$$W_{ai} = 0.4335 \times P^2 - 2.3897 \times P + 10.768 \quad (4.63)$$

$$W_{aib} = 0.4409 \times P^2 - 2.4287 \times P + 10.695 \quad (4.7)$$

The relation between water absorption and compressive strength at 28 days, were analyzed using linear regression as shown in Figure 4-11. The result showed from this scatter that a better correlation obtained between the compressive strength and water absorption. As can be expected, higher water absorption levels at a higher porosity, and thus lower concrete strength. However, the correlation between those two parameters is high (R^2 = 0.8521) and defined as a linear function as shown equation (4.8). This is meant a variation of compressive strength is due to water absorption. In the equation, F_c is compressive strength in MPa and Wa the water absorption (%).

$$F_c = 66.375 - 4.7323 \times Wa \quad (4.8)$$

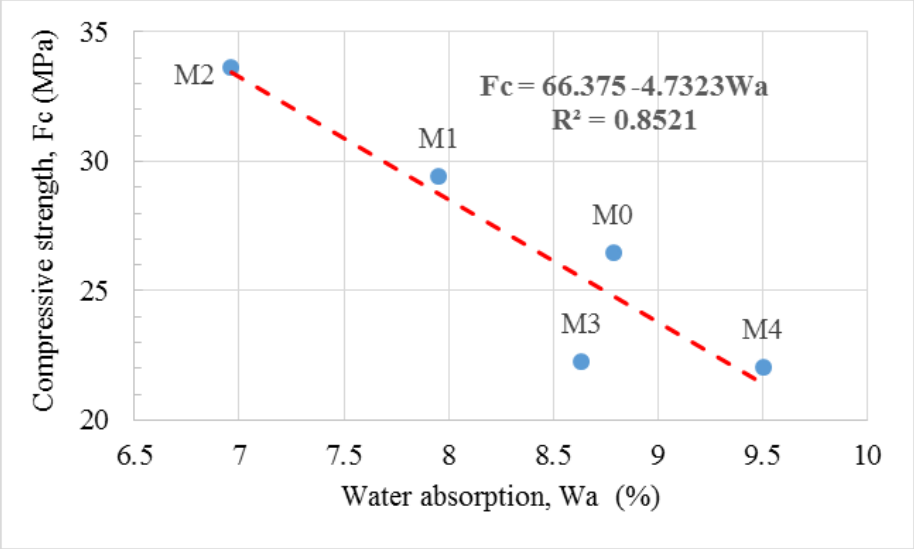

Figure 4-11: Relation between compressive strength and water absorption.

4.3.5 Dry and saturated surface dry density

The results of dry and saturated surface dry are depicted in Figure 4-12. The design wet density was taken to be 2370 kg/m^3. This figure is showing the SSD and dry densities of

the hardened concrete. It is noticed that the average dry density is 2309 kg/m^3 which is below the average normal concrete 2400 kg/m^3.

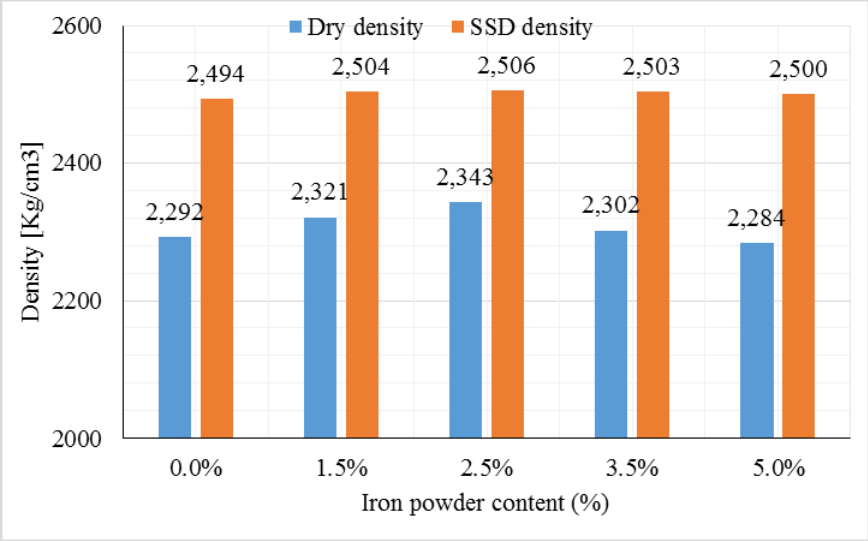

Figure 4-12: Dry and saturated surface dry densities.

4.3.6 Porosity

The results of the porosity in hardened concrete at 28 days are shown in Table 4-10. The porosity of the control specimen (M0) is 19.94%, it starts reducing when the iron powder is added as a concrete component. We noticed that when 1.5 and 2.5% of cement is replaced by iron powder, the porosity decreases by 9.38 and 19.16% respectively. It started increasing when 3.5 and 5% of iron powder is added to the concrete. It is shown that the iron powder is slightly more effective in modifying the pore structures and reducing the porosity of the concrete.

Table 4-9: Porosity of binary blended concrete

Designation	M0	M1	M2	M3	M4
Porosity (%) at 28 days	19.94	18.07	16.12	19.60	21.51

The relationship between the porosity and the amount of iron powder in the concrete is shown in Figure 4-13. This result showed that a certain level of the amount of iron powder, the porosity decreases. This phenomena is due to the fineness particles of iron powder (200 nm) that fill the pore space of the concrete. The coefficient of determination (R^2 = 0.7869) found in the regression analysis shows that the correlation between the two parameters is significant.

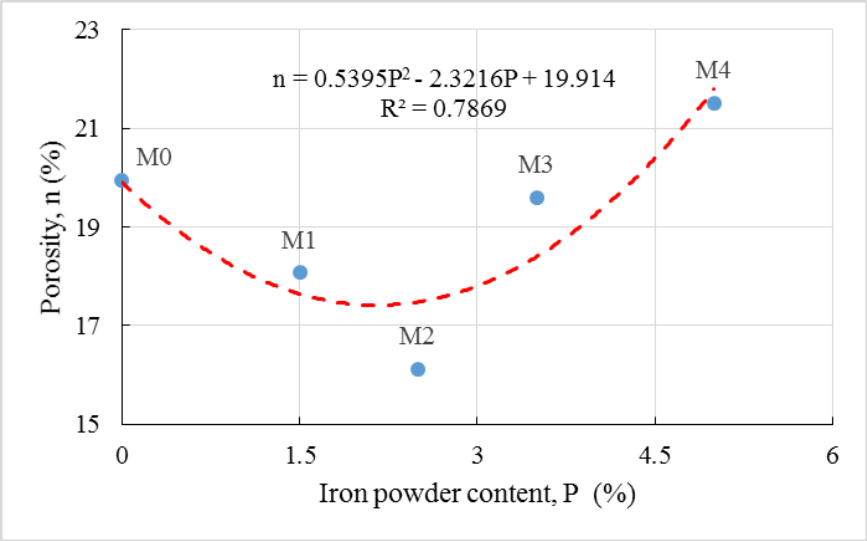

Figure 4-13: Relationship between porosity and the amount of iron powder.

Figure 4-14 is showing the relationship between compressive strength and the porosity. We can notice from the regression curve that higher is the porosity lesser is a compressive strength. The highest value of the compressive which is 33.64 MPa at 2.5% replacement has the lesser percentage of the porosity of 16.12%. As can be seen, from equation (4.9), a linear function was found from regression analysis to correlate the compression strength and the porosity (R^2=0.8498). In the equation, F_c is compressive strength in MPa and n the porosity (%).

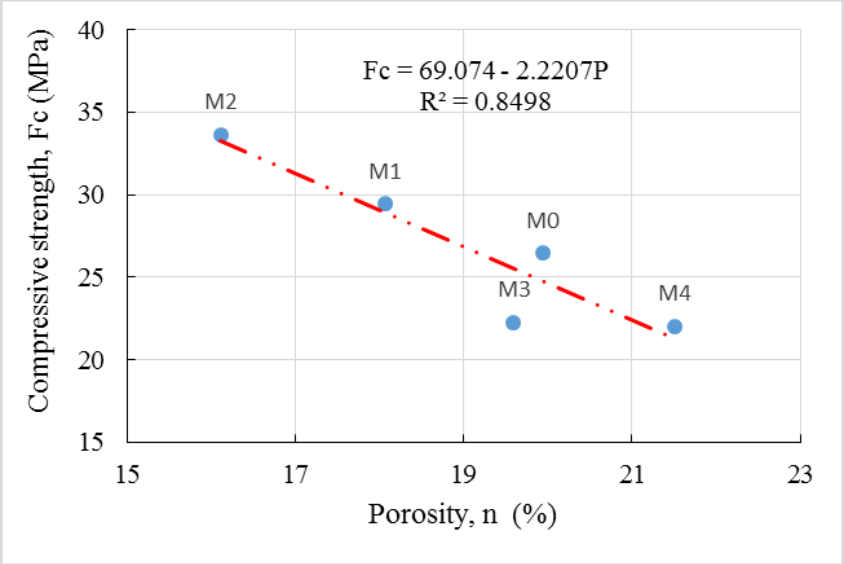

Figure 4-14: Relationship between compressive strength and porosity.

$$F_c = 69.074 - 2.2207 \times n \quad (4.9)$$

The relationship between water absorption and porosity of the iron powder concrete was obtained as shown in Figure 4-15 and equations (4.10) and (4.11). From the regression analysis, it was found that the water absorption increased linearly as the porosity increased. In the equations, Wai is water absorption after immersion (%), Waib is water absorption after immersion and boiling (%), and n the porosity (%).

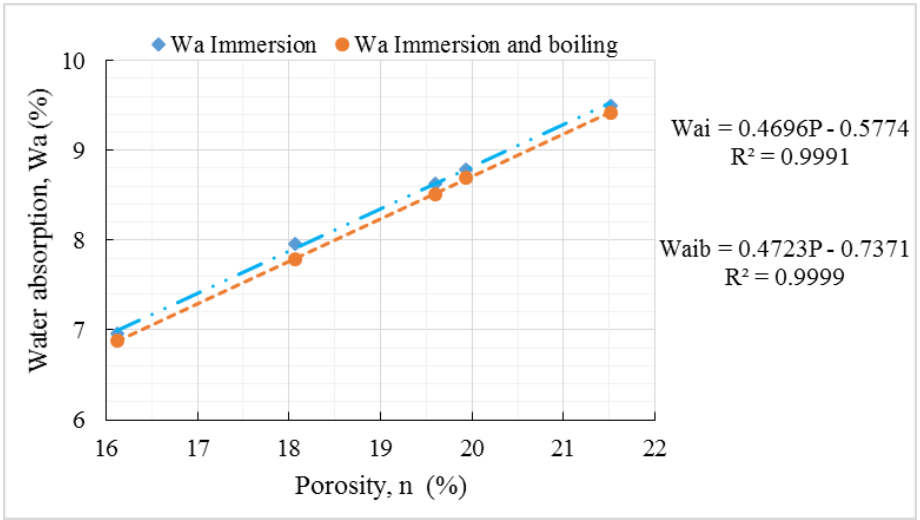

Figure 4-15: Relationship between water absorption and porosity.

$$W_{ai} = 0.4696 \times n - 0.5774 \quad (4.10)$$

$$W_{aib} = 0.4723 \times n - 0.7371 \quad (4.11)$$

4.3.7 Sorptivity

The results of the rate of absorption of the iron powder concrete are shown in Table 4-10. The rate of water absorption ($mm/min^{1/2}$) was found from the slope of the line that is best fit to water absorption (I) plotted versus the square root of time ($min^{1/2}$). The slope was obtained using least squares, linear regression analysis of the plot of I against the square root of time ($t^{1/2}$) as displayed in Appendix 88.

Table 4-10: Sorptivity of the iron powder concrete

Sample	M0	M1	M2	M3	M4
Sorptivity, k ($mm/min^{1/2}$)	0.1312	0.1855	0.1724	0.1757	0.1902
Coefficient of determination (R^2)	0.9928	0.9914	0.9902	0.9928	0.9846
Coefficient of correlation (R)	0.9964	0.9957	0.9951	0.9964	0.9923

4.4 Durability performance

4.4.1 Chloride penetration

In this study, chloride penetration has been investigated at 30, 45, and 60 days and the results found are depicted as shown in Figure 4-16. The white region indicated the depth penetration of chloride, while the yellow region indicated that there were no signs of chloride attack as shown in Figure 4-17. Based on Figure 4-16, 1.5 and 2.5% of replacement of cement by iron powder, the average value of chloride penetration decreased when compared to the control sample. It means the addition of iron powder lessen the diffusion of chloride ion within the concrete and prevent it from reaching the

steel reinforcement. Nevertheless, after 3.5% and 5% of replacement of cement, the chloride depth started increasing.

The relationship between the depth of chloride ingress and the time of exposure in sodium chloride solution was obtained as shown in Figure 4-18. From the regression analysis, it was found that the chloride penetration increased exponentially with the days of exposure, equations (4.12) to (4.16).

$$Pd_0 = 0.8262 \times e^{0.0066d} \quad (4.124)$$

$$Pd_1 = 0.5332 \times e^{0.0112d} \quad (4.13)$$

$$Pd_2 = 0.5699 \times e^{0.0074d} \quad (4.14)$$

$$Pd_3 = 1.1469 \times e^{0.0068d} \quad (4.15)$$

$$Pd_4 = 1.2885 \times e^{0.0073d} \quad (4.16)$$

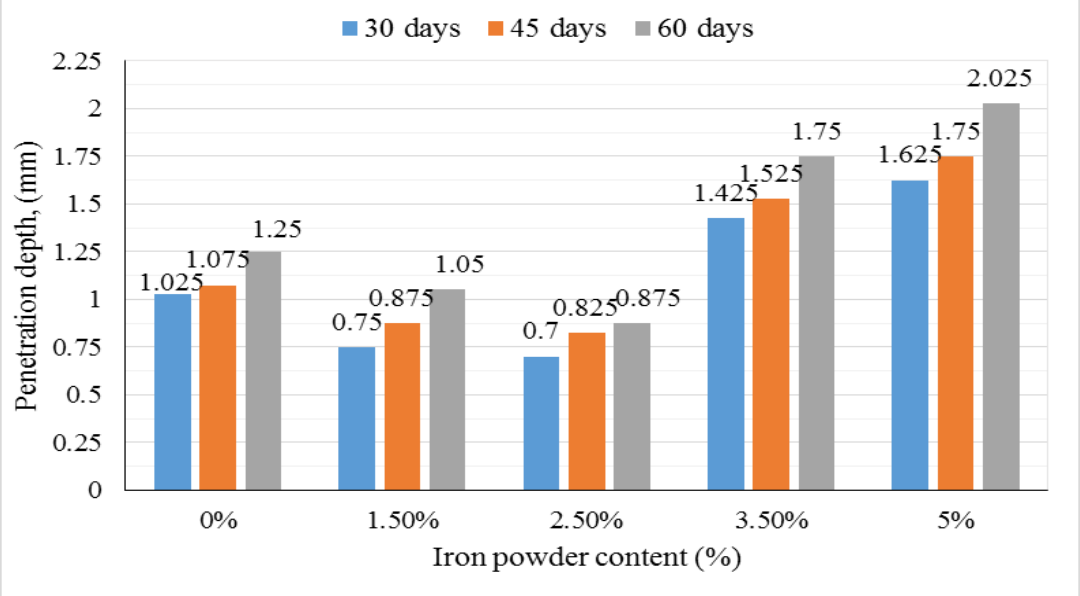

Figure 4-16: Depth of chloride ions penetration versus iron powder content.

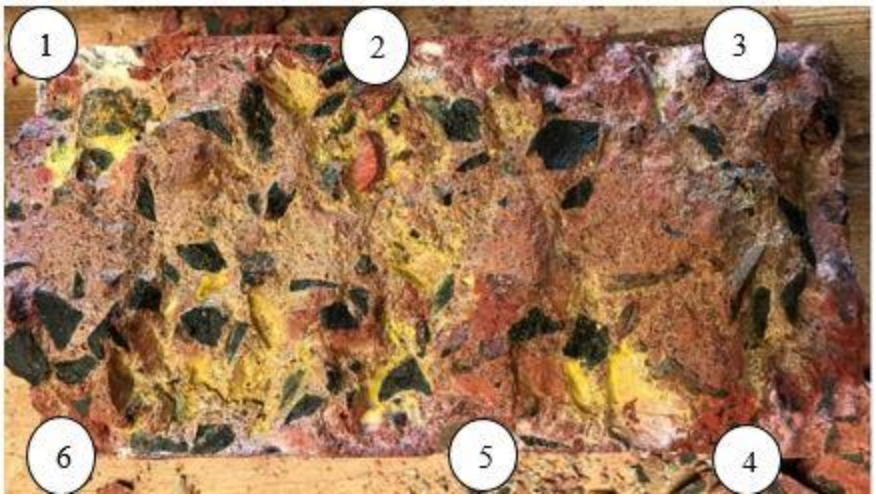

Figure 4-17: Measuring chloride penetration.

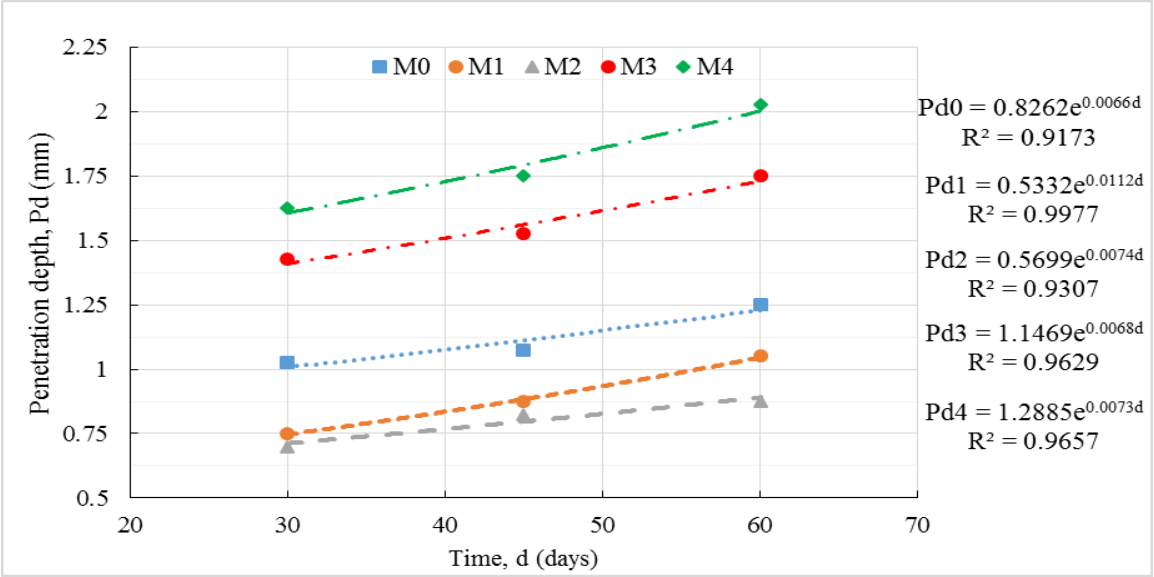

Figure 4-18: Depth of chloride penetration versus days of exposure.

4.4.2 Acid attacks

The acid attacks were investigated in term of weight loss and compressive strength loss. Five concrete mixtures were prepared. The first concrete mix was made without iron powder and the four others with iron powder content in concrete. After 28 days of curing in water, samples were immersed to 2 and 3% of hydrochloric acid solution for a duration of 28, 45 and 60 days. A total of 120 concrete specimen were casted, 90 specimen were

exposed to hydrochloric acid and 30 specimen were cured in water. In order to minimize the evaporation, the specimen were kept covered throughout the testing period. Acid attack resistance was evaluated by determining the weight loss (WL) and compressive strength loss (CSL) of the specimen using equations (4.17) and (4.18). In the equations, W_1 and W_2 are the weights of the specimen (kg) before and after immersion in 2 and 3% of hydrochloric acid solution, F_{c1} is the compressive strength of the specimen cured in water and F_{c2} is the compressive strength of the specimen after exposure to 2 and 3% in hydrochloric acid solution.

$$\mathrm{WL}(\%) = [(\mathrm{W_1} - \mathrm{W_2})/\mathrm{W_1}] \times 100 \quad (4.17)$$

$$\mathrm{CSL}(\%) = [(\mathrm{F_{c1}} - \mathrm{F_{c2}})/\mathrm{F_{c1}}] \times 100 \quad (4.18)$$

4.4.2.1 Weight loss

The weight loss has been studied and the results obtained are depicted as shown in Figure 4-19 for 2% hydrochloric acid exposure and Figure 4-20 for 3% hydrochloric acid solution. The equation (4.19) has been used to calculate the weight loss of the different type of mixture in this study. The result showed that when 1.5 and 2.5% of cement replaced by iron powder the weight loss decreased by remains lesser than the control specimen. The samples containing 3.5 and 5% of the iron powder showed also weight loss decreased but compared to the control specimen, they remain higher. The specimen of all the different mixtures showed more degradation when exposed to 3% hydrochloric acid solution for 28, 45 and 60 days than the one exposed to 2% hydrochloric acid solution for the same duration. The weight losses of the samples were due to the degradation provoked by acid penetration. Acid provoked the external faces of the sample to corrosion.

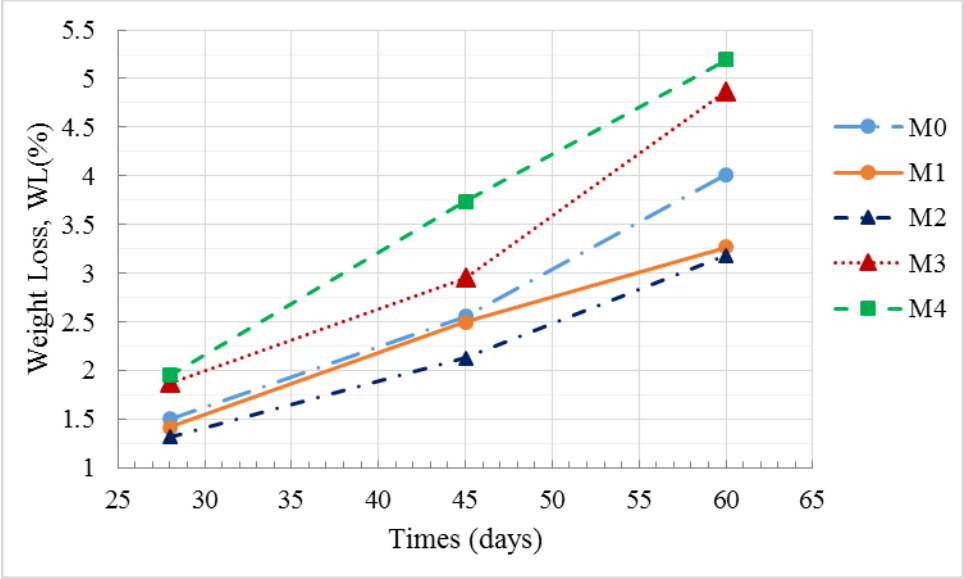

Figure 4-19: Weight loss of the different mixture into 2% hydrochloric acid solution.

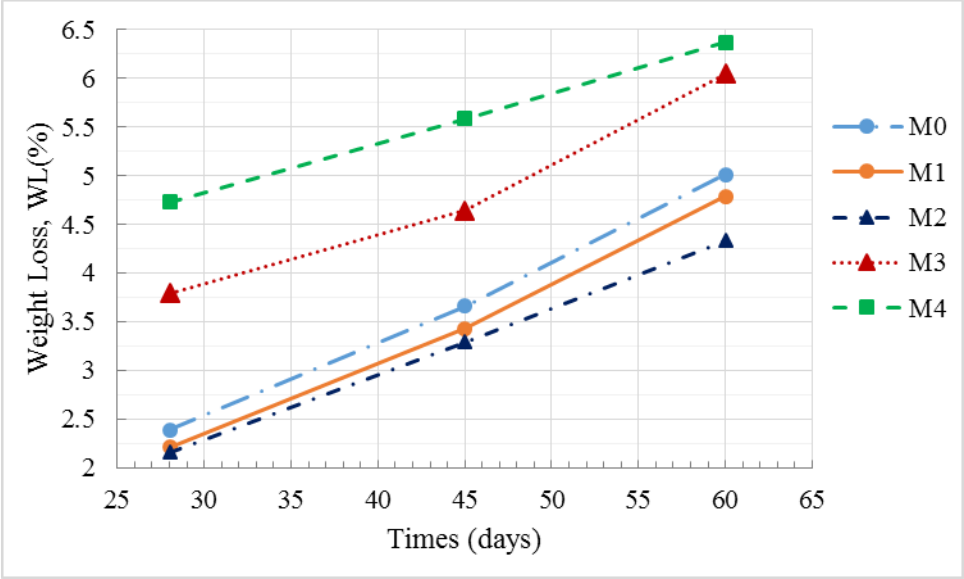

Figure 4-20: Weight loss of the different mixture into 3% hydrochloric acid solution.

4.4.2.2 Compressive strength loss

The influence of hydrochloric acid solution at 2 and 3% when into the water was studied. Test samples are compared with the control samples. This comparison was made with the control samples made cured in water. After 28, 45, and 60 days of exposure to hydrochloric acid solution, the two concrete specimen were tested for residual

compressive strength. The strength loss was determined with reference to the strength of concrete without exposure as shown in Figure 4-21. The compressive strength of the specimen after 28, 45 and 60 days exposure in 2 and 3% hydrochloric acid solution is given in Figure 4-22 and 4-23, respectively. The percentages of compressive strength loss for each specimen are depicted in Figure 4-24 and 4-25. The specimen containing 1.5 and 2.5% iron powder were found more resistant to acid attack than the specimen made with 3.5 and 5% iron powder replacement, as regards to the compressive strength loss throughout the testing period (28, 45 and 60 days). The specimen exposed to 3% hydrochloric acid solution showed more compressive strength loss compared to 2% hydrochloric acid solution exposure.

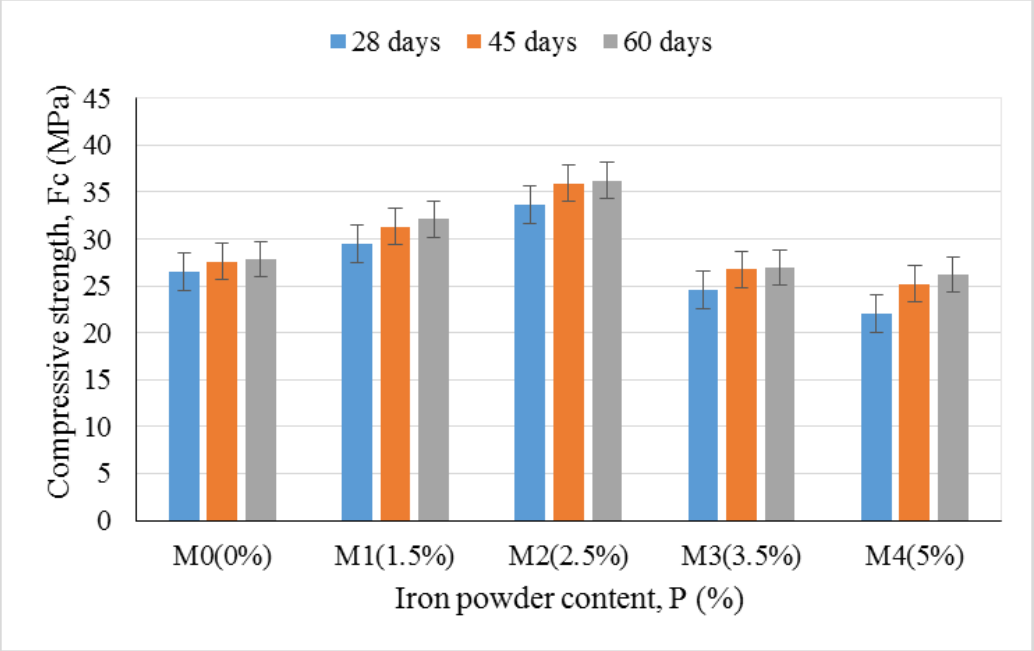

Figure 4-21: Compressive strength at different days of curing in water.

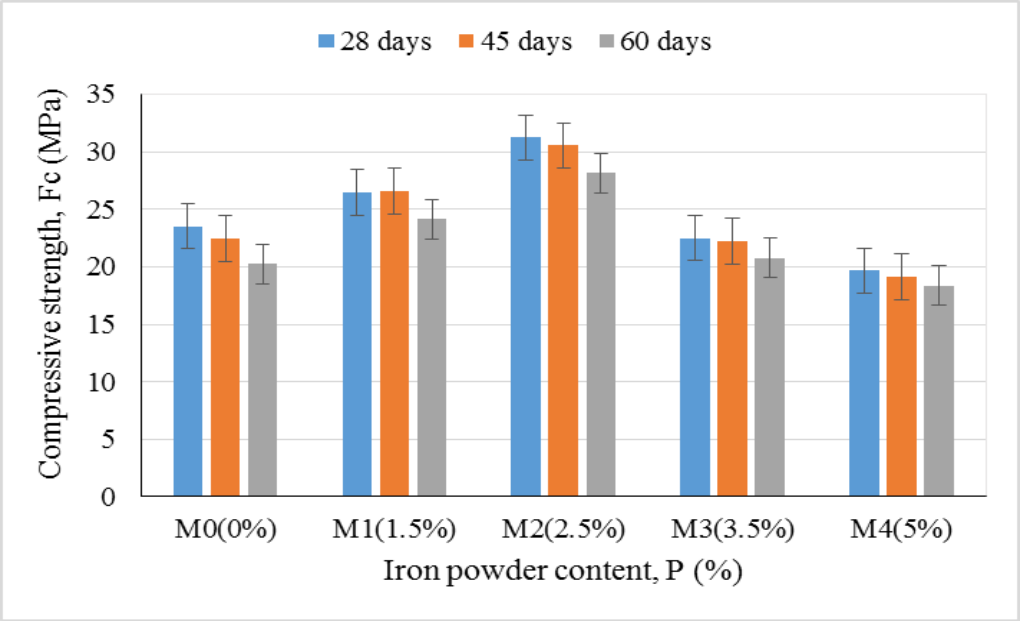

Figure 4-22: Compressive strength at different days in 2% hydrochloric acid solution.

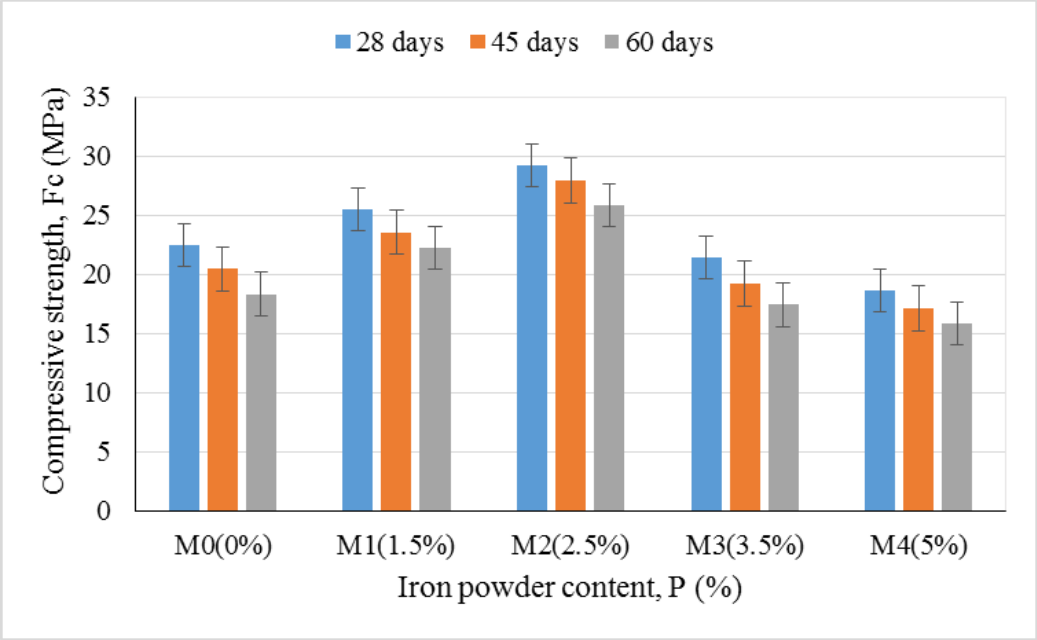

Figure 4-23: Compressive strength at different days in 3% hydrochloric acid solution.

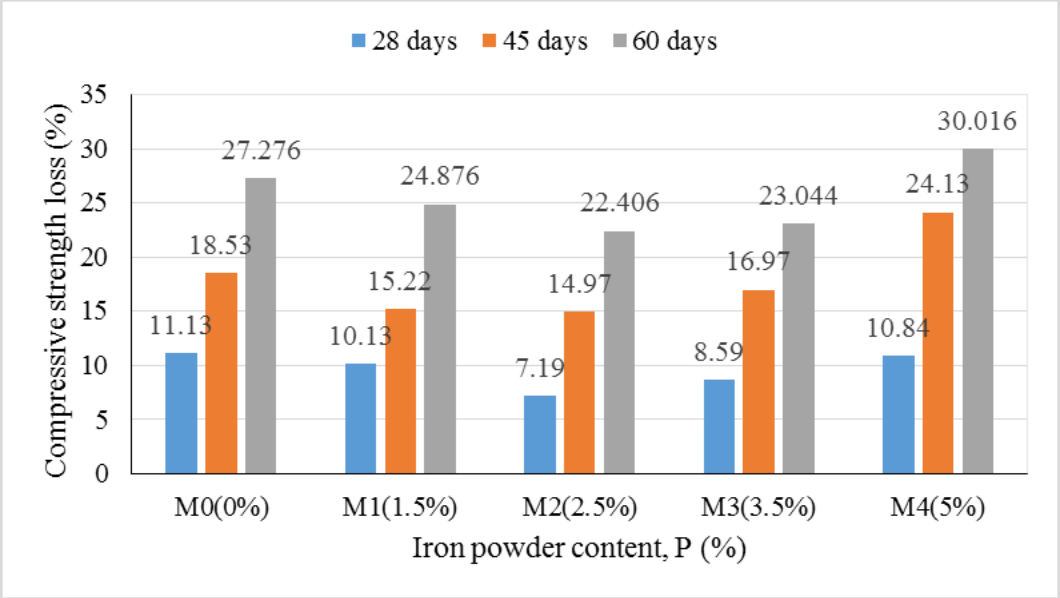

Figure 4-24: Compressive strength loss at different days in 2% hydrochloric acid solution.

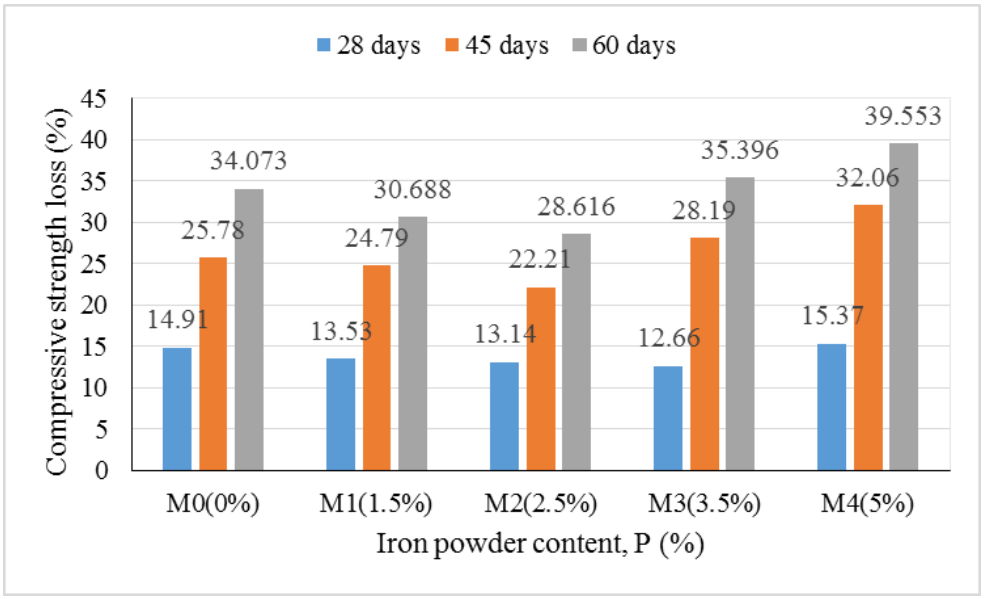

Figure 4-25: Compressive strength loss at different days in 3% hydrochloric acid solution.

4.5 Structural Performance of Concrete Beams

4.5.1 None-reinforced concrete beam

The flexural strength of the none-reinforced concrete (NRC) beam was carried out according to BS 1881 part 118. A total of 6 beams were casted and tested after 28 days. The NRC beam of dimension 150 mm x 150 mm x 550 mm were tested using a UTM with a maximum load capacity of 2000 kN. The load was applied as stroke control loading with a loading rate of 0.025 MPa (Figure 4-26). Before loading, strain gauges with a length of 60 mm each used in the flexural test. These were glued on the tensile surfaces of the concrete beam specimen to measure the tensile strain. The flexural strength and maximum load results of the series NRC-B0 and NRC-B1 are shown in Table 4-11. From result obtained, when 2.5% of iron powder replaced by Portland cement, the flexural strength increased by 18.22% at 28 days.

Table 4-11: Flexural strength at 28 days of two different non-reinforced beam

Specimen	Maximum load (kN)	Maximum flexural strength (MPa)
NRC-B0 (Control)	29.912	3.988
NRC-B1 (2.5% iron powder)	35.366	4.715

The failure of both types of beams NRC-B0 and NRC-B1 occurred roughly under a weak load due to lack of tensile strength of the concrete as shown in Figure 4-27 and 4-28 which relate load and time of loading. Typical load-strain curves recorded from a tension test are shown in Figure 4-29. It is evident that the two tensile-strain values of the two type of concretes measured on opposite faces of the beams are very close up to about 50 to 70% of the failure load.

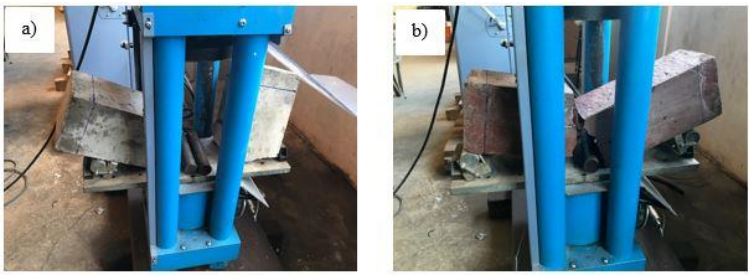

Figure 4-26: Crack pattern at ultimate failure a) NRC-B0 and b) NRC-B1 specimen.

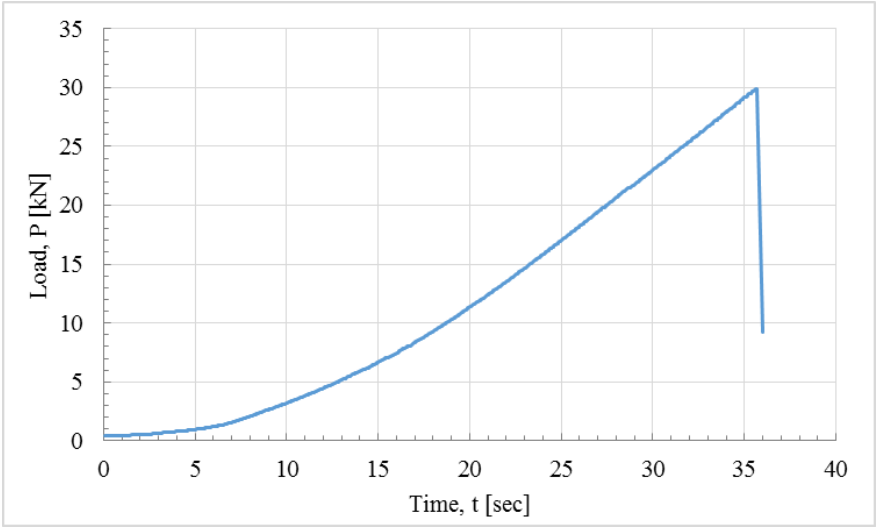

Figure 4-27: Load versus time of the NRC-B0 specimen.

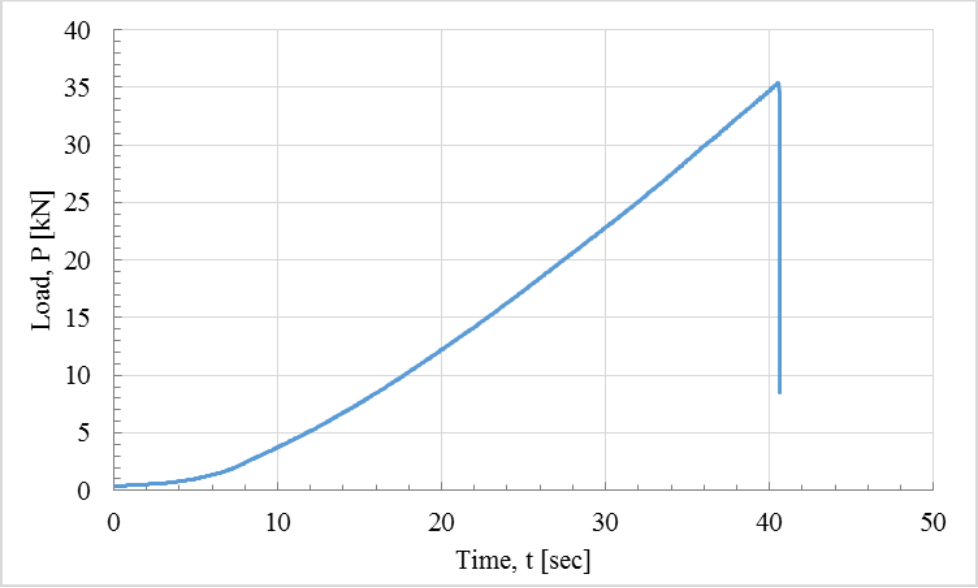

Figure 4-28: Load versus time of the NRC-B1 specimen.

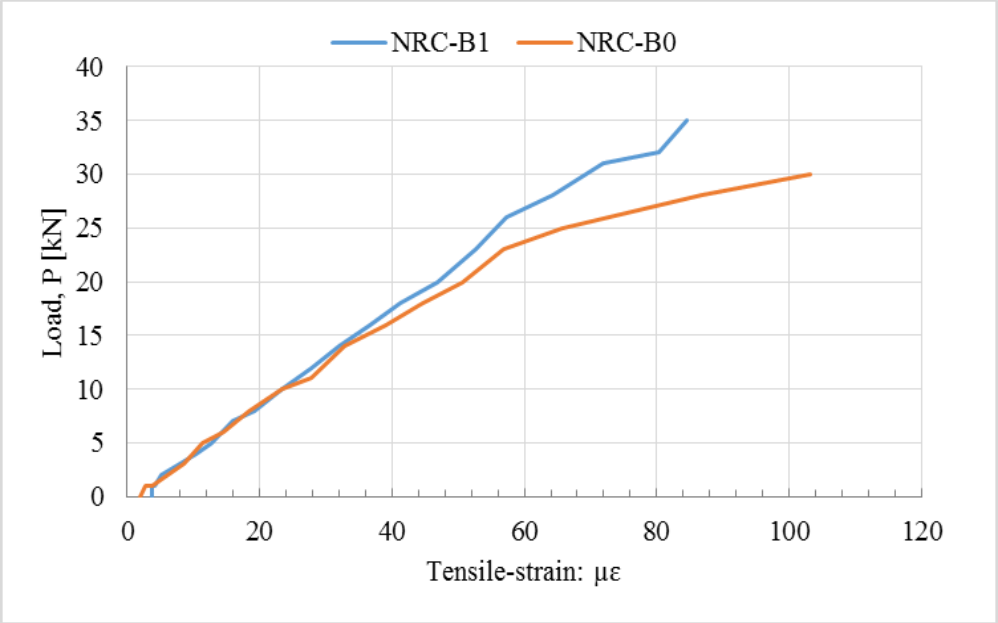

Figure 4-29: Typical Load-strain curves of the concrete in tensile.

4.5.2 Reinforced concrete beam

A total of six specimen of 150 mm x 150 mm 1000 mm of dimensions were tested after 28 days from casting. The specimen were reinforced with two 10 mm diameter rib bars (Y10) as tensile reinforcement, two 8 mm diameter rid bars (Y8) as compressive reinforcement and 6 mm diameter shear stirrups (R6) with 150 mm spacing. RC beam specimen with hinge-roller supports were tested using a frame testing machine as shown in Table 4-13. The load was applied as stroke control loading using a hydraulic jack and load cell to report the loading rate. Before loading, a strain gauge was attached at the bottom surface of the concrete beam to measure the tensile strain. To obtain an accurate deflection reading, a Linear Variable Differential Transducer (LVDT) was mounted at the mid-span. Crack initiation and propagation were monitored by visual inspection during testing, and the crack patterns were marked.

Table 4-12: First crack, ultimate loads and moments for RC-B0 and RC-B1

Designation	First crack load (kN)	First crack moment (kN.m)	Ultimate load (kN)	Ultimate moment (kN.m)
RC-B0	69	10.35	85	12.75
RC-B1	74	11.1	89	13.35

4.5.2.1 First crack and failure load

The first crack in both sets of beams appeared approximately at 15 to 35 mm from the mid span at the region of maximum moment; then, followed by diagonal cracks from the points of loading towards the supports. The crack openings were larger in RC-B0 beams than in RC-B1 beams; this was an indicator of the fact that the presence of iron powder in the concrete matrix can effectively control the cracks. Figure 4-30 shows region of pure shear and pure bending along the loaded beam for a given P. The first crack and failure loads for all beam specimen are listed in

Table 4-12. It was also noticeable that with RC-B0 beam specimen, the first crack appeared suddenly and propagated relatively faster until failure, than with RC-B1 Beam specimen; RC-B1 beams exhibited less brittle failure. However, the first crack loads and the failure loads for RC-B1 Beam specimen were found slightly greater than for RC-B0 beam specimen. The onset of failure was first noticed in the tension zone of the beams (at the bottom) by the cracking of concrete.

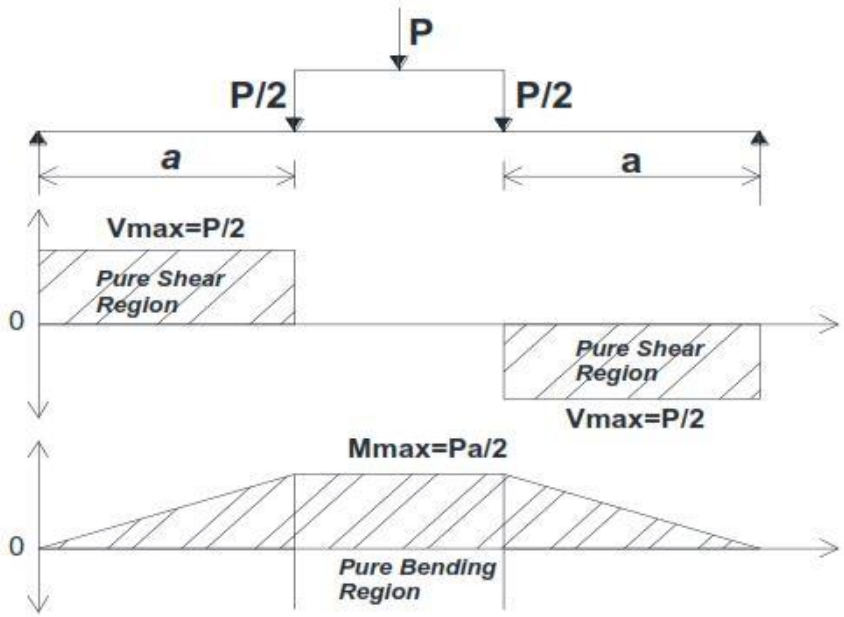

Figure 4-30: Shear force and bending moment diagrams for a beam under four points loads.

The failure loads of both beams specimen RC-B0 and RC-B1 can be seen in

Table 4-12. From the value, the RC-B1 beams can be as structurally efficient as RC-B0 beams or even better, since RC-B1 beams could sustain more loads at higher failure strains than that for RC-B0 beams, due to iron powder which controlled cracks and acted as cracks arresters.

4.5.2.2 Failure mode and cracks patterns

The failure mode observed was both the diagonal tension failure and flexural failure. The failure started at the bottom part of the beams in the tension zone, by the cracking of concrete due to high flexural tensile stresses greater than the tensile strength of the beams. This is a flexural type of failure; it can also be due to the compression stresses causing the crushing of the extreme fibers in compression at the top of beams. Then,

inclined cracks appeared and propagate diagonally in the shear span; this is a diagonal tension failure, due to high shear stresses. Diagonal tension failure type can be due to inadequate shear reinforcements. Before the yielding of tensile reinforcement, initiation of cracks occurred earlier in the concrete specimen with iron powder also in the specimen without iron powder. Figure 4-31 shows the crack pattern and failure modes of the beam specimen.

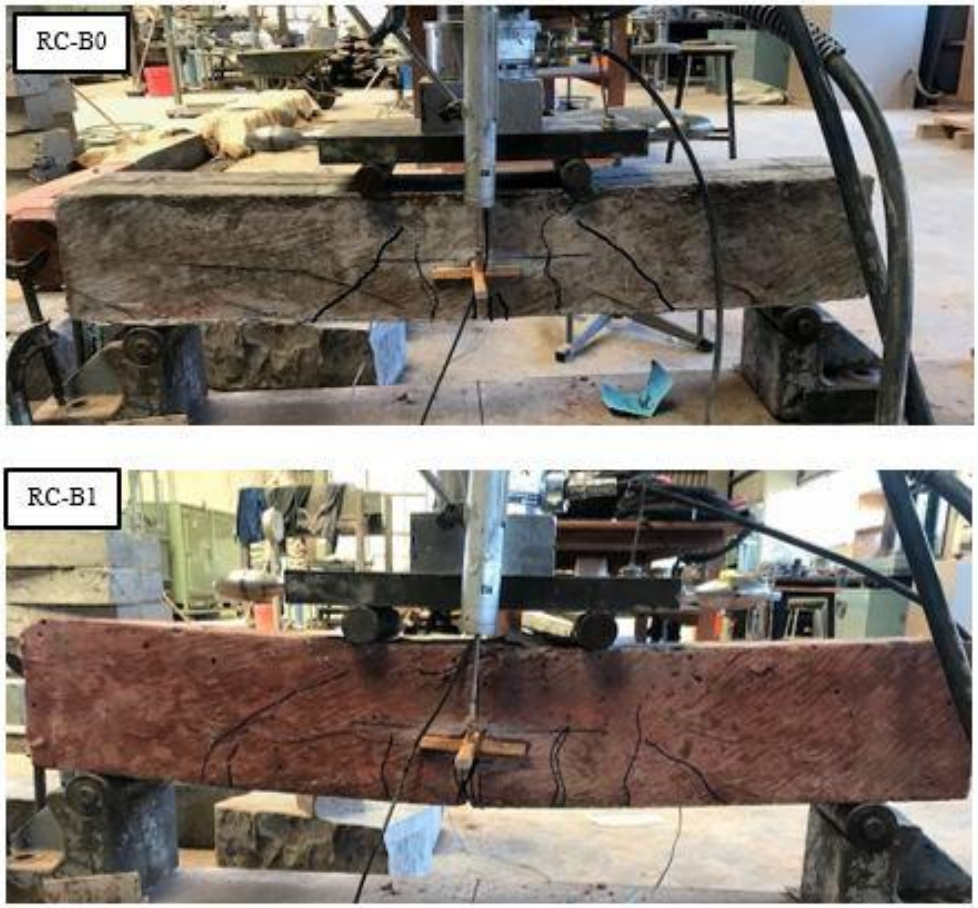

Figure 4-31: Crack patterns and failure mode of different beams specimen.

4.5.2.3 Deflection of beams

The measured load-deflection relations from the RC beam tests are shown in Figure 4-32. The results showed that the elastic behavior of all specimen before cracking was similar

even though the RC-B1 specimen content 2.5% of iron powder. The curves showed basically three main phases regarding the load-deflection during the test. In the first phase, as the load increased, the deflection also increased; this can be seen as the elastic phase. Then, came the second phase where the deformations were still increasing for almost constant loads and finally started to decrease until complete failure of the beams specimen, this was the last phase.

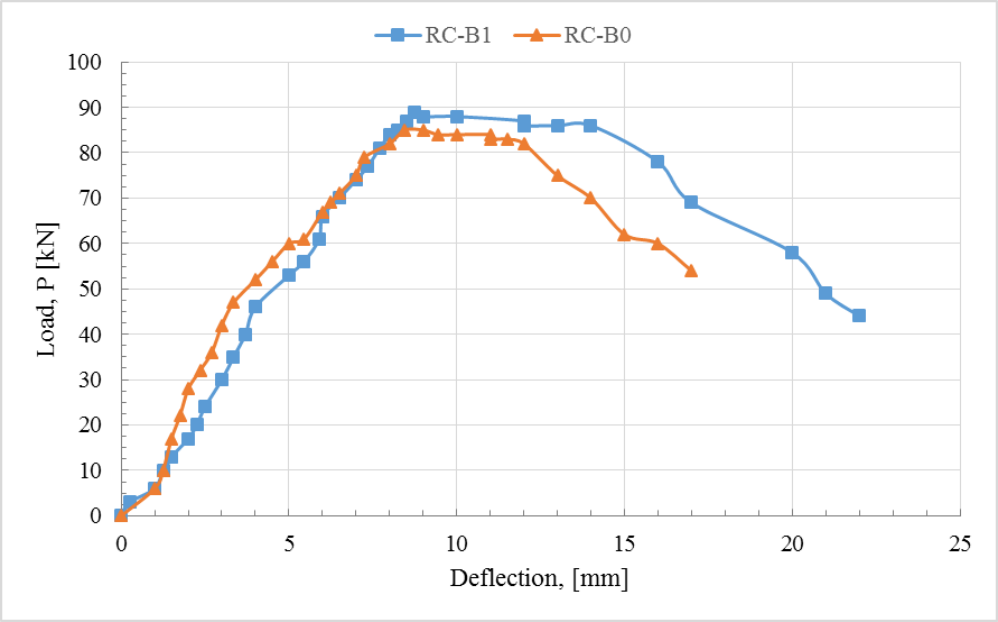

Figure 4-32: Load-deflection curves of different specimen at the age of 28 days.

British Standard BS 8110 provides a recommendation regarding the allowable deflection which should be less or equal to beam span divided by 250. Figure 4-33 shows the maximum mid-span deflections of the beam specimen at service load. For both RC-B0 and RC-B1 beams, the values of maximum deflection recorded are higher than the allowable and the deflection of RC-B1 beam specimen is 29.41% higher than the deflection of RC-B0 beam specimen. This can be explained by the higher ductility of RC-B1 beam specimen. It is noticeable from the load mid-span deflections curves shown in

Figure 4-33 that the value of 3.6 mm representing the allowable deflection falls in the elastic domain. This is because the standards recommend designing structures in the elastic phase of deformations for safety purposes. The values given by Figure 4-33 are the maximum deflection that occurs.

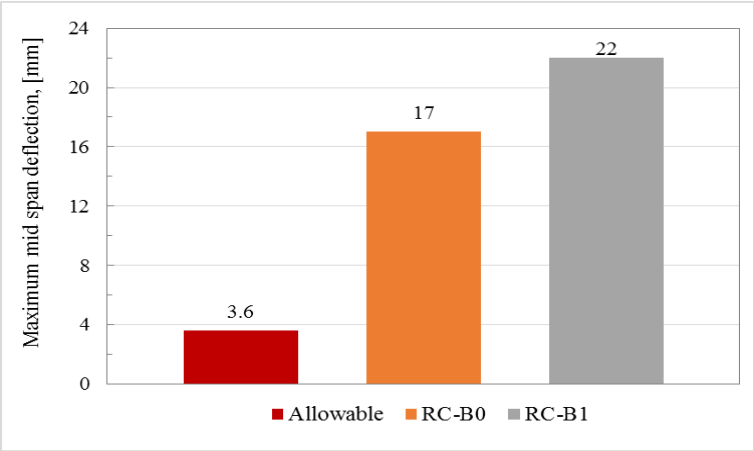

Figure 4-33: Experimental and allowable maximum mid-span deflection for different specimen.

4.5.2.4 Ultimate moment and curvatures

Figure 4-34 shows the cross-section of the reinforced concrete beam that was used to determine the moment of inertia and the neutral axis. Modulus of elasticity of concrete is a key factor for estimating the deformation of structural elements, as well as a fundamental factor for determining the modular ratio, n, which is used for the design of structural members subjected to flexure.

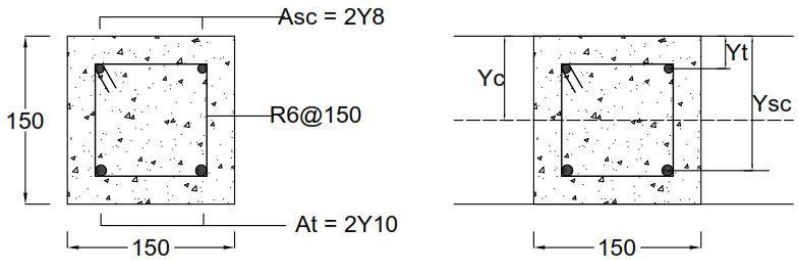

Figure 4-34: Cross-section of the reinforced beam.

According to (Group, n.d.), the modulus of elasticity of concrete can be estimated from the specified characteristic strength as in equation (4.20). In the equation, Ec is the modulus of elasticity (MPa) of a concrete at the age of 28 days, f_c is the characteristic strength (MPa) of the concrete, Eco is equal to 20500 MPa, and α_E is a constant parameter depending on the aggregate type, generally taken equal to 1.0.

$$Ec = Eco \times \alpha_E\left((f_c + 8)/10\right)^{1/3} \quad (4.20)$$

From equation (4.20), the modulus of elasticity of the control concrete specimen is 30,970.12 MPa and for the concrete containing 2.5% of iron powder replacement of cement is 32,980.52 MPa. The young modulus of steel being 200,000 MPa, we can express the modular ration n as:

$$n = \frac{Es}{Ec} \quad (4.21)$$

This coefficient allows estimating the equivalent section of steel reinforcements in concrete section. For the control concrete n=6.46 and n=6.06 for the concrete with 2.5% iron powder content. The neutral axis is given by:

$$Y = \frac{\sum A_i Y_i}{\sum A_i} = \frac{A_c Y_c + (n-1)A_{sc} Y_{sc} + (n-1)A_t Y_t}{A_c + (n-1)A_{sc} + (n-1)A_t} \quad (4.22)$$

In equation (4.22), Asc is steel reinforcements in compression (mm^2), At is steel reinforcements in tension (mm^2), Ac is the concrete area (mm^2), and Yc, Ysc, and Yt are the distances from the center of gravity of each section to the top compression fiber. For the control concrete n=6.46, Y = 7.56 cm and n=6.06 Y = 7.55 cm for the concrete with 2.5% iron powder content. The moment of inertia I of the section is given by equation (4.23). In the equation, Ii, Ai, and di are respectively the moment of inertia of the element

about its neutral axis, the distance from its neutral axis to the neutral axis of the whole section and the area of the element.

$$I = \sum(I_i + A_i d_i^2) = \sum\left[\left(\frac{bh^3}{12} + bhd_c^2\right) + (n-1)A_{sc}d_{sc}^2 + (n-1)A_t d_t^2\right] \quad (4.23)$$

The moment of inertia I of the section was found equal to 4 508.5726 cm^4 for the control specimen, and equal to 4 487.3402 cm^4 for the concrete with 2.5% iron powder content. According to the authors, the Poisson ratio ν of the concrete ranges between 0.14 and 0.26. However, the average value ν = 0.20 meets the required accuracy for the design of elements subjected to cracks formation at the ultimate limit state. The moment-curvature curves of RC-B0 and RC-B1 beam specimen are shown in Figure 4-35.

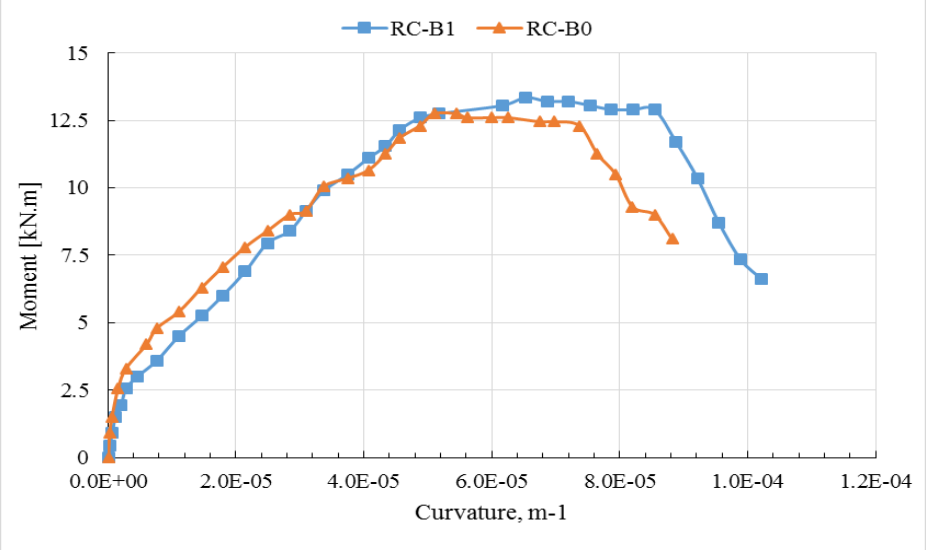

Figure 4-35: Moment-curvature curves for different beam specimen.

The experimental moment was calculated for each applied load P using equation (4.24) in which a is the shear span.

$$M = \frac{Pa}{2} \quad (4.24)$$

The curvature is given by equation (4.25) where ξ is the extreme compression fiber strain corresponding to each load P and a section curvature, and "c" the compression depth or the distance of the top compression fiber from the neutral axis.

$$Ø = \frac{\xi}{c} \tag{4.25}$$

The strains were obtained at mid-span of the beams with the strains gauges, and then used to calculate the curvature Ø. The curves show almost similar behaviors for the two beam specimen. However, RC-B1 beam specimen exhibit greater curvatures than S beam specimen. This can be easily explained by the presence of iron powder in the concrete matrix of RC-B1 beam specimen, which makes the beams more elastic and ductile.

4.5.2.5 Flexural stress-strain behavior

Flexure formula is given by equation (4.26) where σ is the flexural stress, M is the maximum bending moment, Y is the depth of the neutral axis or the distance between the neutral axis and the top fiber of the section, and I is the moment of inertia about the neutral axis of the section.

$$\sigma = \frac{MY}{I} \tag{5}$$

The flexural strain is a nominal fractional change in the length of an element of the outer surface of the specimen at the middle of the span, where the maximum strain occurs. It is given by equation (4.27) in which D is the maximum deflection of the center of the beam (mm), L the length of the support span (mm) and, d is the thickness of the beam (mm).

$$\xi f = \frac{6Dd}{L^2} \tag{6.27}$$

Figure 4-36 shows the flexural stress-strain curves for RC-B0 and RC-B1 beam specimen. The curves show almost similar trends in the stress-strain relationship.

However, RC-B1 beam specimen show greater ability to resist deformation under load than RC-B0 beam specimen. This means that the flexural strength of RC-B1 beam specimen is higher than the one of RC-B0 beam specimen as depicted in Figure 4-36. This higher ability can be attributed to the iron powder in the concrete matrix of RC-B1 Beam specimen, which improves the tensile strength of the concrete while controlling the cracks leading to a higher ability to resist deformations under load.

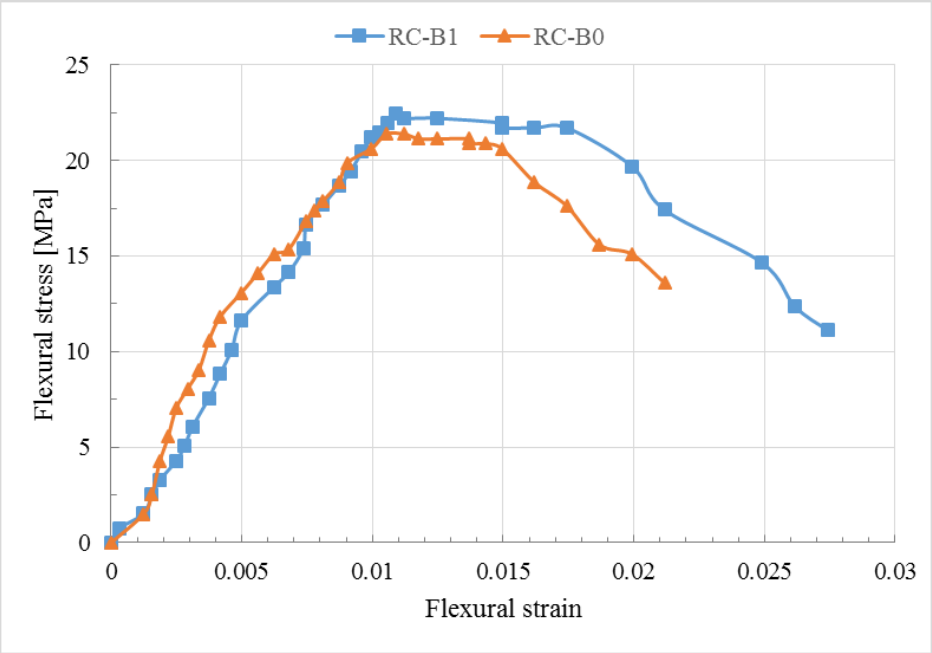

Figure 4-36: Flexural stress-strain curves of different beam specimen.

CHAPTER FIVE

5 CONCLUSIONS AND RECOMMENDATIONS

5.1 Conclusions

From the experiments carried out and based on the results obtained on the "Effect of Iron powder partially used as cement replacement on the physical and mechanical properties of concrete exposed to chemical attacks", some conclusions can be drawn:

i) In this study, the materials used were characterized by grading analysis, specific gravities, densities, water absorption, void content and chemical composition. From the chemical analysis results obtained iron powder were found to be 88% pure and the cement Portland was found to be good quality for concrete production with 63.36% of calcium oxide and 20.62% of silicon dioxide. Both fine and coarse aggregates were well graded.

ii) The physical, mechanical properties of concrete were evaluated by partially replacement of cement up to 5%. A total of five mixes containing 1.5, 2.5, 3.5 and 5% of iron red powder have been investigated. Iron powder increased compressive and tensile strengths of concrete in comparison of the concrete without iron powder. It is found advantageous if cement replaced by iron powder up to a maximum limit of 2.5% with predominant particles of 200 nm. The porosity decreased when 1.5 and 2.5% of cement is replaced by iron powder, then start increasing but still remained less than the control specimen.

iii) Durability performance through acid attack resistance tests and chloride penetration resistance test of the concrete specimen were assessed for a period of 28, 45 and 60 days. The specimen of all the different mixtures showed more

degradation when exposed to 3% hydrochloric acid solution than the one exposed to 2% hydrochloric acid solution for the same duration. However the samples with 2.5% cement replacement was found to be more resistant to the penetration of chloride throughout the testing period, with the lowest value of penetration depth of 0.7 mm, 0.825 mm, and 0.875 mm at 28, 45, and 60 days as compared to 1.025 mm, 1.075 mm and 1.25 mm for the control specimen (concrete without iron powder) for the same period.

iv) Structural performance through non reinforced and reinforced concrete beams were evaluated. Based on experimental results, both reinforced and non-reinforced concrete beam with 2.5% of iron powder had higher flexural strength than those made without iron powder. Reinforced concrete beam with iron powder were able to sustain more loads with higher failure strains than the beam without iron powder. The first crack loads for reinforced concrete beam with 2.5% of iron powder were found to be 6.75% slightly greater than the reinforced concrete beam without iron powder. However the reinforced concrete beam with and without iron powder revealed similar failure mode and crack patterns as shown in Figure 4-31.

5.2 Recommendations

From this work and its findings, some recommendations can be suggested for an eventual future study to ascertain the use of iron powder into concrete in the construction industry:

i) To extend compressive strength test after 90 days and 1 year to follow the strength development with time regardless of compressive, splitting tensile and flexural tests;

ii) Durability study was carried out in this study over a period of 60 days only. Further experiments should be done over a longer period such as 90 days and more; To execute durability tests such as chemical resistance, chloride penetration, freeze/thaw resistance, stain resistance, deep abrasion resistance, crazing resistance, thermal shock resistance, Warpage, wedging, bond strength, breaking strength, thermal expansion, and moisture expansion;

iii) The scanning electron microscopy (SEM) should be investigated to show the microscopy form and evaluate the porosity.

iv) This research study was mainly based on the experimental works. However, for a deeper understanding of the material behaviors, a finite element modeling need to be carried out. This can be done using finite element software such as Castem or ABAQUS. The aim would be to analyze the structural responses of the material, calibrated on the experimental results obtained in the laboratory. Thereafter, assess the structural capacity of various bearing elements under various combination of load types (horizontal loads, vertical loads, and dynamic loads), carry out analysis on the nonlinear behaviors of various structural elements made with the specimen in terms of their capacity curves, assess the cracks patterns, enlighten the deformation behaviors modes under loading, observe and analyze the damage mechanisms on structural elements.

REFERENCES

Ahmed, M. A., Hassanean, Y. A., Assaf, K. A., & Shawkey, M. A. (2015). The Effect of Incorporation of Ferrite Nanoparticles on Compressive Strength and Resistivity of Self-Compacting Concrete, (March), 131–138.

Arefi, M. R., & Rezaei-zarchi, S. (2012). Synthesis of Zinc Oxide Nanoparticles and Their Effect on the Compressive Strength and Setting Time of Self-Compacted Concrete Paste as Cementitious Composites, 4340–4350. https://doi.org/10.3390/ijms13044340

ASTM C1585-13. (2013). Standard Test Method for Measurement of Rate of Absorption of Water by Hydraulic-Cement Concretes. *ASTM International*, *41*(147), 1–6. https://doi.org/10.1520/C1585-13.2

ASTM C642-13. (2013). *Standard Test Method for Density, Absorption, and Voids in Hardened Concrete*.

Edward G. Nawy. (June 2008). Concrete Construction Engineering Handbook, 2nd edition.

Bassuoni, M. T., & Nehdi, M. L. (2007). Resistance of self-consolidating concrete to sulfuric acid attack with consecutive pH reduction. *Cement and Concrete Research*, *37*(7), 1070–1084. https://doi.org/10.1016/j.cemconres.2007.04.014

Branch, Y., & Branch, T. (2011). To study the effect of adding Fe 2 O 3 nanoparticles on the morphology properties and microstructure of cement mortar, *8*(4), 2–6.

British Standard Institution. (2013). *BS 1881-125 Testing concrete. Methods for mixing and sampling fresh concrete in the laboratory*.

British Standard Institution BSI (1881). (1881). Part 115: Specification for compression testing machines for concrete.

British Standard Institution BSI (1996). (1996). Standard Specification for Portland Cement. *Bs En 12:1996*, (May), 1–9.

British Standards Institution. (1983). *Testing concrete Part 103. Method for determination of compacting factor*.

British Standards Institution. (2014). BSI Standards Publication BS EN 206 Concrete — Specification, performance, production, and conformity. *Bsi*, (May).

British Standards Institutions. (1983). *Testing concrete. Method for determination of tensile splitting strength*.

BS 8500-1. (2015). Complementary to BS EN 206-2; Part 2: Specification for constituent materials and concrete, 1–33. Retrieved from http://shop.bsigroup.com/en/ProductDetail/?pid=000000000030133680

Chen, X., Wu, S., & Zhou, J. (2013). Influence of porosity on compressive and tensile strength of cement mortar. *Construction and Building Materials*, *40*(August 2016), 869–874. https://doi.org/10.1016/j.conbuildmat.2012.11.072

Dai, J., Wang, J., Sangregorio, C., Fang, J., Carpenter, E., & Tang, J. (2000). Benefits of Fe2O3 nanoparticles in concrete mixing matrix, *87*(10), 7397–7399. https://doi.org/10.1002/adma.201603730

Ghannam, S., Najm, H., & Vasconez, R. (2016). Experimental study of concrete made with granite and iron powders as partial replacement of sand. *Sustainable Materials*

and Technologies, *9*, 1–9. https://doi.org/10.1016/j.susmat.2016.06.001

Hall, C. (1989). Water sorptivity of mortars and concretes: a review. *Magazine of Concrete Research*, *41*(147), 51–61. https://doi.org/10.1680/macr.1989.41.147.51

Hanus, M. J., & Harris, A. T. (2013). Nanotechnology innovations for the construction industry. *Progress in Materials Science*, *58*(7), 1056–1102. https://doi.org/10.1016/j.pmatsci.2013.04.001

Javier, A. R. A., Lopez, N. E., & Juanzon, J. B. P. (2017). Compressive Strength and Chloride Penetration Tests of Modified Type IP Cement Concrete with Rice Ash. *Procedia Engineering*, *171*, 543–548. https://doi.org/10.1016/j.proeng.2017.01.369

Kumar, R., & Bhattacharjee, B. (2003). Porosity, Pore Size Distribution and In-situ Strength of Concrete. *Cement and Concrete Research*, *33*(1), 155–164. https://doi.org/10.1016/S0008-8846(02)00942-0

Li, H., Xiao, H. G., Yuan, J., & Ou, J. (2004). Microstructure of cement mortar with nano-particles. *Composites Part B: Engineering*, *35*(2), 185–189. https://doi.org/10.1016/S1359-8368(03)00052-0

Madandoust, R., Mohseni, E., Mousavi, S. Y., & Namnevis, M. (2015). An experimental investigation on the durability of self-compacting mortar containing nano-SiO2, nano-Fe2O3and nano-CuO. *Construction and Building Materials*, *86*, 44–50. https://doi.org/10.1016/j.conbuildmat.2015.03.100

Mendes, T., Hotza, D., & Repette, W. (2015). Nanoparticles in Cement-Based Materials: a Review. *Reviews on Advanced Material Science*, *40*, 89–96. Retrieved from

http://www.ipme.ru/e-journals/RAMS/no_14015/06_14015_mendes.pdf

Mohapatra, M., & Anand, S. (2010). Synthesis and applications of nano-structured iron oxides/hydroxides – a review. *International Journal of Engineering, Science and Technology*, *2*(8), 127–146. https://doi.org/10.4314/ijest.v2i8.63846

Nazari, A., Riahi, S., Riahi, S., Shamekhi, S. F., & Khademno, A. (2010). Influence of Al2O3 nanoparticles on the compressive strength and workability of blended concrete. *Journal of American Science*, *6*(5), 6–9.

Neville, A. M. (2011). *Properties of Concrete*. https://doi.org/10.4135/9781412975704.n88

Olar, R. (2011). Nanomaterials and Nanotechnologies for Civil Engineering. *"Bulletin of the Polytechnic Institute of Iasi - Construction & A*, *61*(4), 109–117.

Ollivier, J. P., & Massat, M. (1992). Permeability and microstructure of concrete: a review of modeling. *Cement and Concrete Research*, *22*(2–3), 503–514. https://doi.org/10.1016/0008-8846(92)90094-C

Oltulu, M., & Şahin, R. (2013). Effect of nano-SiO2, nano-Al2O3 and nano-Fe2O3 powders on compressive strengths and capillary water absorption of cement mortar containing fly ash: A comparative study. *Energy and Buildings*, *58*, 292–301. https://doi.org/10.1016/j.enbuild.2012.12.014

P. Elizabeth. (1992). Nanotechnology yields transparent magnet-tiny iron oxide particles become more transparent than in bulk form. *Science News*, (July 11).

Ponce, J. M., & Batic, O. R. (2006). Different manifestations of the alkali-silica reaction

in concrete according to the reaction kinetics of the reactive aggregate. *Cement and Concrete Research*, *36*(6), 1148–1156. https://doi.org/10.1016/j.cemconres.2005.12.022

Rattan, A., Sachdeva, P., & Chaudhary, A. (2016). Use of Nanomaterials in Concrete. *International Journal of Latest Research in Engineering and Technology*, *02*(05), 81–84. Retrieved from http://www.ijlret.com/Papers/Vol-2-issue-5/14-B2016270.pdf

Sikora, P., Horszczaruk, E., Cendrowski, K., & Mijowska, E. (2016). The Influence of Nano-Fe3O4 on the Microstructure and Mechanical Properties of Cementitious Composites. *Nanoscale Research Letters*, *11*(1), 182. https://doi.org/10.1186/s11671-016-1401-1

Soleymani, F. (2012). Computer-Aided Prediction of Physical and Mechanical Properties of High Strength Concrete Containing Fe2O3 Nanoparticles. *The Journal of American Science, 8, 338-345.*

Sreeram K.J., Indumathy R., Rajaram A., N. B. U. and R. T. (2006). Template synthesis of highly crystalline and monodisperse iron oxide pigments of nanosize. *Materials Research Bulletin*, *Vol.41*, *No*, 1875–1881.

Standard, E. (2000). *Cement - Part 1: Composition, specifications and conformity criteria for common cements*.

Stanish, K. D., Hooton, R. D., & Thomas, M. D.. (1997). Testing the Chloride Penetration Resistance of Concrete : A Literature Review. *Prediction of Chloride Penetration in Concrete*, 31.

Thomas, M. (2011). The effect of supplementary cementing materials on alkali-silica reaction: A review. *Cement and Concrete Research*, *41*(12), 1224–1231. https://doi.org/10.1016/j.cemconres.2010.11.003

Zongjin Li, C. L., & Xi, and Y. (2009). *Structural Renovation in Concrete*.

APPENDICES

Appendix 1: Mix Design Calculations

Calculations of mix design proportions:

The assumptions considered for the determination of the mix proportions were:

- Characteristic compressive strength is 25 N/mm2 at 28 days with 2.5% defectives
- Slump required was 30 to 60 mm
- Nominal maximum aggregate 20 mm (uncrushed)
- Fine aggregate 60% passing 600 µm sieve (uncrushed)
- Water-free / cement ratio 0.5
- Minimum cement content 300 Kg
- Standard deviation s = 8
- The constant of 2.5% defectives k = 1.96

Proportioning design with this method is articulated broadly on 5 main steps as follows:

Step 1: The required strength leading to the w/c ratio

Calculation of the mean strength

$$f_m = f_c + M$$

Where: Margin M = k * s, f_m is the target mean strength, f_c is the specific characteristic strength and, s is the standard deviation taken to equal 8.

Calculation of current margin:

$$M = \mathrm{k} \times \mathrm{s}$$

$$M = 1.96 \times 8$$

$$\boldsymbol{M = 15.68\ MPa}$$

Calculation of the target mean strength:

$$f_m = f_c + M$$

$$f_m = 25 + 15.68$$

$$\boldsymbol{f_m = 40.68\ \text{MPa}}$$

The target mean strength calculated, is used to determine the w/c ratio.

Table 3-2 gives the strength depending on 0.5 w/c, and the type of the cement and aggregate. The mean strength calculated, allowed us to choose the approximate compressive strength at 28 days 42 MPa for a water-cement ratio 0.5, the aggregate is uncrushed and the cement type is ordinary Portland cement.

Step 2: The workability leading to the free water content

The slump required was 30 to 60 mm.

Table 3-3 gives free water content in kg/m^3 required to give various levels of workability.

Here, the water content equal to 180 kg/m^3(table 3-3)

Step 3: Step 1 and step 2 leading to obtain the cement content

$$\frac{\mathrm{W}}{\mathrm{C}} = 0.5 \quad \rightarrow \quad \mathrm{C} = \frac{\mathrm{W}}{0.5}$$

$$\mathrm{C} = \frac{180}{0.5} = 360\ \mathrm{kg/m^3}$$

The cement content is greater than the minimum cement content, hence we consider **C = 360 kg/m^3**

Step 4: determination of the total aggregate content.

Wet density of concrete = density of water + density cement + density of total aggregate

Density of total aggregate = Wet density of concrete – (density of water + density cement)

Appendix 3 gives the relationship between the free water content and the wet density of concrete.

We plotted the free water content and found the wet density of concrete equal to 2370 kg/m^3

Density of total aggregate = 2370 – (180 +360) = 1830

Density of total aggregate = 1830 kg/m^3

Step 5: The selection of the fine and coarse aggregate contents

The nominal maximum aggregate size is 20 mm, the fine aggregate passing 600 µm is 60%. Appendix 5 gives the relationship between free-water/cement ratio and the proportion of fine aggregate (%) for maximum size 20 mm.

We plotted the w/c ratio and found there is 32 % of fine into the total aggregate amount.

Density of fine aggregate = 0.32 x 1830

Density fine aggregate = 585. 6 kg/m^3

Density of coarse aggregate = density of total aggregate – density of fine aggregate

Density of coarse aggregate = 1830 – 585.6

Density of coarse aggregate = 1244.4 kg/m^3

Step 6: Estimation of the theoretical unit weight (per m^3 of concrete)

Cement 360 kg

Water 180 kg

Sand 585.6 kg

Coarse 1244.4 kg

Appendix 2: Compressive and Split Tensile Strength

Mechanical properties	Compressive strength(Mpa)			Tensile strength(MPa)		
	7 days	14 days	28 days	7 days	14 days	28 days
M0 (0%)	15.58	23.09	26.48	1.75	2.00	2.16
M1 (1.5%)	23.08	24.32	29.44	1.86	2.03	2.26
M2 (2.5%)	25.50	29.77	33.64	1.65	1.92	2.09
M3 (3.5%)	15.39	22.08	24.59	1.63	1.80	2.02
M4 (5%)	15.06	19.90	22.06	1.51	1.61	1.87

Appendix 3: Relation between Compressive Strength and Water/Cement Ratio

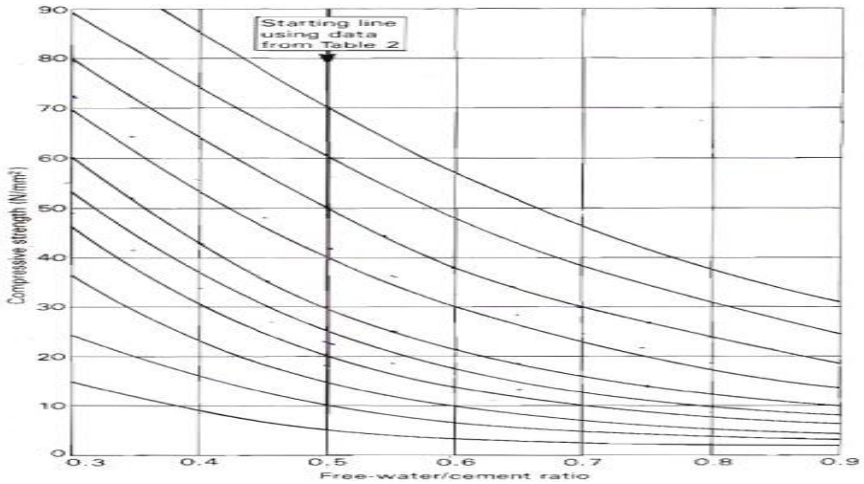

Appendix 4: Relation between Free-Water Content and Wet Density of Concrete Mix

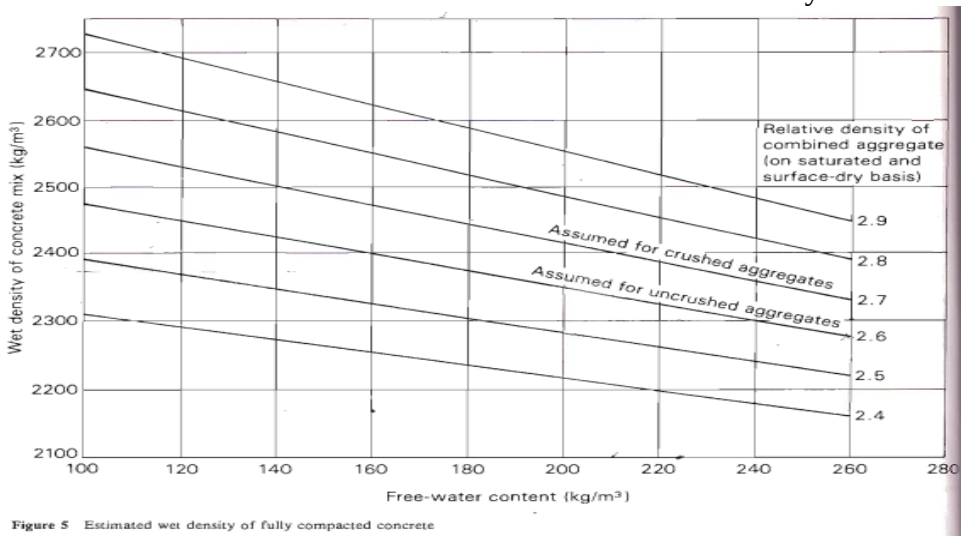

Figure 5 Estimated wet density of fully compacted concrete

Appendix 5: Free-Water/ Cement Ratio and Proportion Fine Aggregate (%) for Maximum Size 10 mm

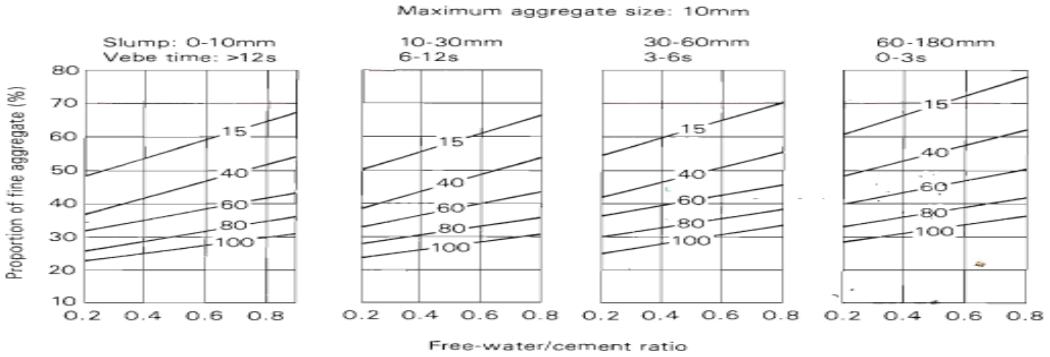

Figure 6 Recommended proportions of fine aggregate according to percentage passing a 600 μm sieve

Appendix 6: Free-Water/ Cement Ratio and Proportion Fine Aggregate (%) for Maximum Size 20 mm

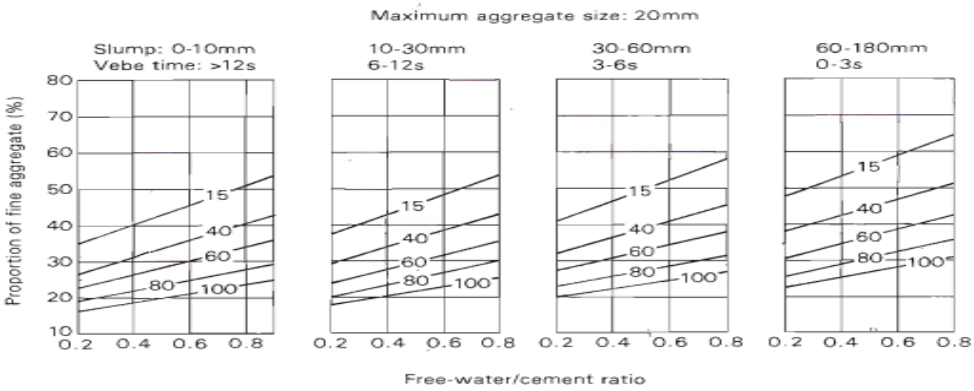

Appendix 7: Free-Water/ Cement Ratio and Proportion Fine Aggregate (%) for Maximum Size 40 mm

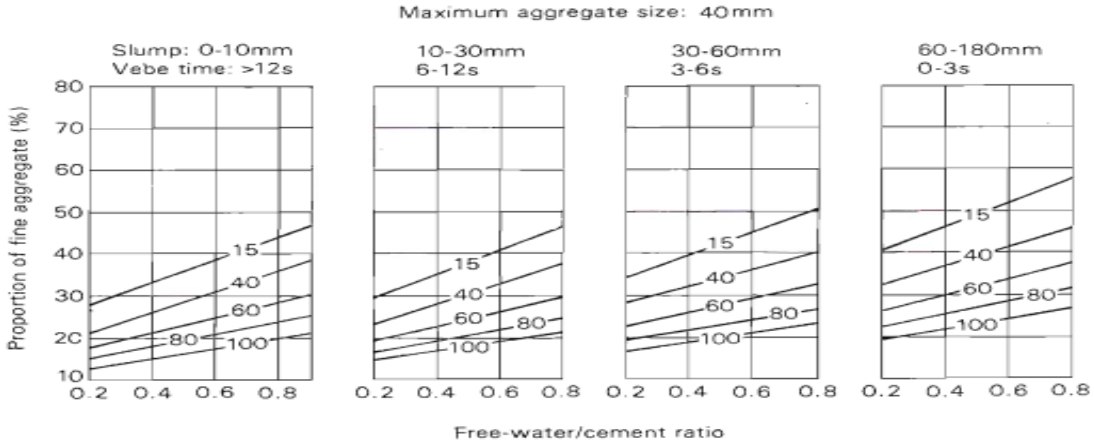

Appendix 8: Cumulative Water Absorption versus Square Root of Time

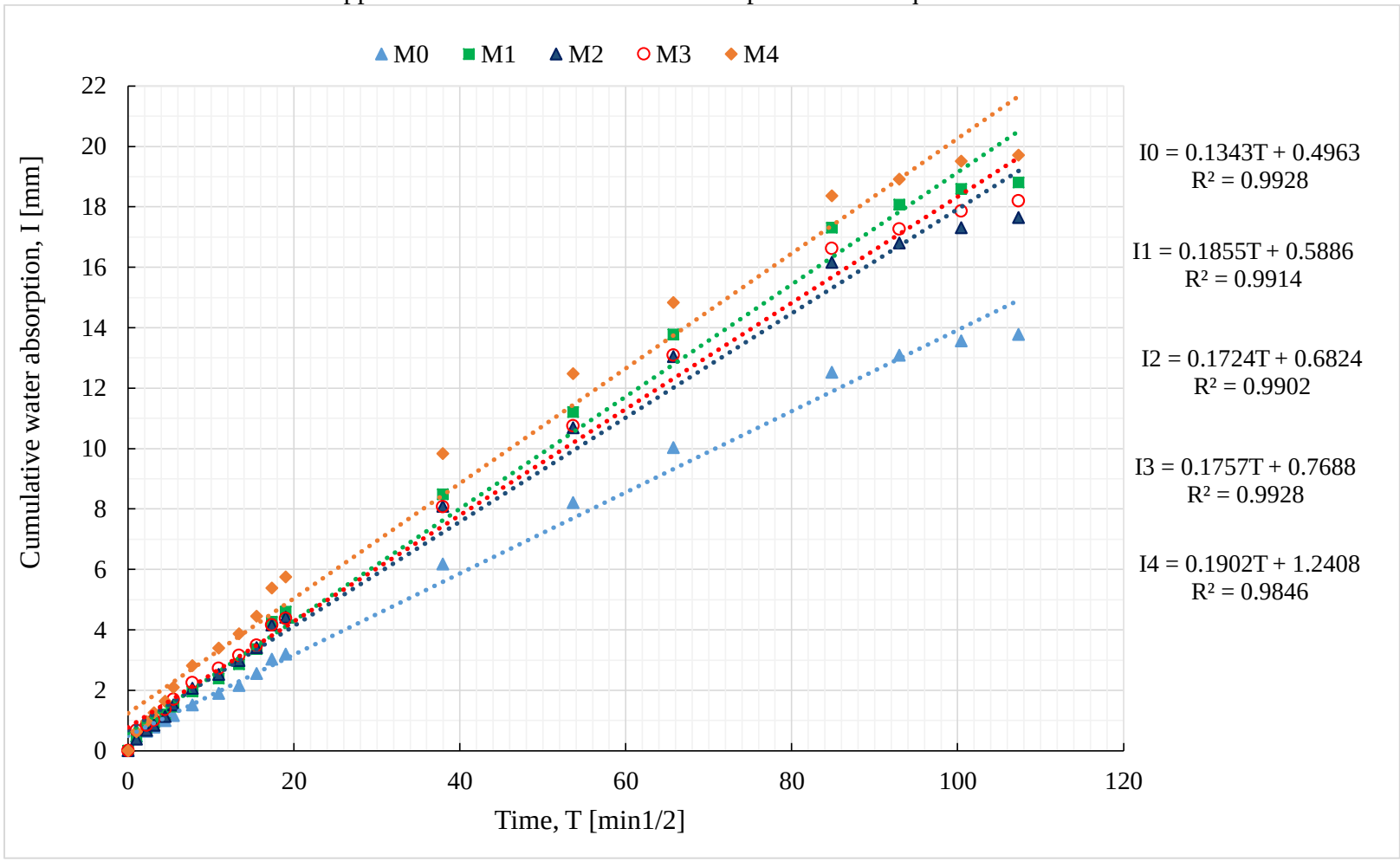

Appendix 9: Load Raw Deflection Data

RC-B0 beam specimen's data

Load (kN)	0	3	6	10	13	17	20	24	30	35	40	46	53	56	61	66
Deflection (mm)	0	0.25	1	1.25	1.5	2	2.25	2.5	3	3.35	3.7	4	5	5.45	5.9	6

70	74	77	81	84	85	87	89	88	88	87	86	86	86	78	69	58	49	44
6.5	7	7.35	7.7	8	8.25	8.5	8.75	9	10	12	12	13	14	16	17	20	21	22

RC-B1 beam specimen's data

Load (kN)	0	6	10	17	22	28	32	36	42	47	52	56	60	61	67
Deflection (mm)	0	1	1.25	1.5	1.75	2	2.35	2.7	3	3.35	4	4.5	5	5.45	6

69	71	75	79	82	85	85	84	84	84	83	83	82	75	70	62	60	54
6.25	6.5	7	7.25	8	8.45	9	9.45	10	11	11	11.5	12	13	14	15	16	17

Appendix 10: Strain Rosette Data and Processing
RC-B0 beam specimen's data

Strain gauge A	Strain gauge B	Moment M=Pa/2	I=4508.5726 Y=7.56	Curvature	Flexural stress	Flexural strain
0.000E+00	4.695E-07	0.000E+00	5.964E+02	6.210E-08	0.000E+00	0.000E+00
4.695E-07	1.878E-06	9.000E-01	5.964E+02	2.484E-07	1.509E+00	1.246E-03
1.408E-06	4.695E-06	1.500E+00	5.964E+02	6.210E-07	2.515E+00	1.557E-03
1.878E-06	1.174E-05	2.550E+00	5.964E+02	1.553E-06	4.276E+00	1.869E-03
1.268E-05	2.113E-05	3.300E+00	5.964E+02	2.795E-06	5.533E+00	2.180E-03
5.117E-05	4.554E-05	4.200E+00	5.964E+02	6.024E-06	7.043E+00	2.491E-03
8.216E-05	5.775E-05	4.800E+00	5.964E+02	7.638E-06	8.049E+00	2.927E-03
1.131E-04	8.357E-05	5.400E+00	5.964E+02	1.105E-05	9.055E+00	3.363E-03
1.441E-04	1.108E-04	6.300E+00	5.964E+02	1.466E-05	1.056E+01	3.737E-03
1.751E-04	1.352E-04	7.050E+00	5.964E+02	1.789E-05	1.182E+01	4.173E-03
2.061E-04	1.620E-04	7.800E+00	5.964E+02	2.142E-05	1.308E+01	4.983E-03
2.371E-04	1.883E-04	8.400E+00	5.964E+02	2.490E-05	1.409E+01	5.606E-03
2.681E-04	2.146E-04	9.000E+00	5.964E+02	2.838E-05	1.509E+01	6.228E-03
2.991E-04	2.338E-04	9.150E+00	5.964E+02	3.093E-05	1.534E+01	6.789E-03
3.300E-04	2.549E-04	1.005E+01	5.964E+02	3.372E-05	1.685E+01	7.474E-03
3.610E-04	2.831E-04	1.035E+01	5.964E+02	3.745E-05	1.735E+01	7.785E-03
3.920E-04	3.075E-04	1.065E+01	5.964E+02	4.068E-05	1.786E+01	8.097E-03
4.230E-04	3.277E-04	1.125E+01	5.964E+02	4.335E-05	1.886E+01	8.720E-03
4.540E-04	3.446E-04	1.185E+01	5.964E+02	4.558E-05	1.987E+01	9.031E-03
5.643E-04	3.685E-04	1.230E+01	5.964E+02	4.875E-05	2.062E+01	9.965E-03
6.746E-04	3.854E-04	1.275E+01	5.964E+02	5.098E-05	2.138E+01	1.053E-02
7.850E-04	4.113E-04	1.275E+01	5.964E+02	5.440E-05	2.138E+01	1.121E-02
8.953E-04	4.249E-04	1.260E+01	5.964E+02	5.620E-05	2.113E+01	1.177E-02
1.006E-03	4.540E-04	1.260E+01	5.964E+02	6.005E-05	2.113E+01	1.246E-02
1.030E-03	4.728E-04	1.260E+01	5.964E+02	6.254E-05	2.113E+01	1.370E-02

1.054E-03	5.103E-04	1.245E+01	5.964E+02	6.750E-05	2.088E+01	1.370E-02
1.077E-03	5.272E-04	1.245E+01	5.964E+02	6.974E-05	2.088E+01	1.433E-02
1.101E-03	5.573E-04	1.230E+01	5.964E+02	7.371E-05	2.062E+01	1.495E-02
1.125E-03	5.784E-04	1.125E+01	5.964E+02	7.651E-05	1.886E+01	1.619E-02
1.149E-03	6.000E-04	1.050E+01	5.964E+02	7.937E-05	1.761E+01	1.744E-02
1.173E-03	6.197E-04	9.300E+00	5.964E+02	8.197E-05	1.559E+01	1.869E-02
1.197E-03	6.460E-04	9.000E+00	5.964E+02	8.545E-05	1.509E+01	1.993E-02
1.221E-03	6.667E-04	8.100E+00	5.964E+02	8.818E-05	1.358E+01	2.118E-02

RC-B1 beam specimen’s data

Strain gauge A	Strain gauge B	Moment M=Pa/2	I=4487.3402 Y=7.55	Curvature	Flexural stress	Flexural strain
4.695E-07	4.695E-07	0.000E+00	5.943E+02	6.218E-08	0.000E+00	0.000E+00
1.408E-06	1.878E-06	4.500E-01	5.943E+02	2.487E-07	7.571E-01	3.114E-04
1.878E-06	5.164E-06	9.000E-01	5.943E+02	6.840E-07	1.514E+00	1.246E-03
1.268E-05	8.451E-06	1.500E+00	5.943E+02	1.119E-06	2.524E+00	1.557E-03
5.117E-05	1.549E-05	1.950E+00	5.943E+02	2.052E-06	3.281E+00	1.869E-03
1.362E-04	2.113E-05	2.550E+00	5.943E+02	2.798E-06	4.290E+00	2.491E-03
1.958E-04	3.474E-05	3.000E+00	5.943E+02	4.602E-06	5.048E+00	2.803E-03
2.554E-04	5.775E-05	3.600E+00	5.943E+02	7.649E-06	6.057E+00	3.114E-03
3.150E-04	8.357E-05	4.500E+00	5.943E+02	1.107E-05	7.571E+00	3.737E-03
3.746E-04	1.108E-04	5.250E+00	5.943E+02	1.468E-05	8.833E+00	4.173E-03
4.343E-04	1.352E-04	6.000E+00	5.943E+02	1.791E-05	1.010E+01	4.609E-03
4.939E-04	1.620E-04	6.900E+00	5.943E+02	2.145E-05	1.161E+01	4.983E-03
5.535E-04	1.883E-04	7.950E+00	5.943E+02	2.494E-05	1.338E+01	6.228E-03
6.131E-04	2.146E-04	8.400E+00	5.943E+02	2.842E-05	1.413E+01	6.789E-03
6.728E-04	2.338E-04	9.150E+00	5.943E+02	3.097E-05	1.539E+01	7.349E-03
7.324E-04	2.549E-04	9.900E+00	5.943E+02	3.377E-05	1.666E+01	7.474E-03

7.920E-04	2.831E-04	1.050E+01	5.943E+02	3.750E-05	1.767E+01	8.097E-03
8.516E-04	3.075E-04	1.110E+01	5.943E+02	4.073E-05	1.868E+01	8.720E-03
9.113E-04	3.277E-04	1.155E+01	5.943E+02	4.340E-05	1.943E+01	9.156E-03
9.709E-04	3.446E-04	1.215E+01	5.943E+02	4.564E-05	2.044E+01	9.592E-03
1.031E-03	3.685E-04	1.260E+01	5.943E+02	4.881E-05	2.120E+01	9.965E-03
1.090E-03	3.911E-04	1.275E+01	5.943E+02	5.180E-05	2.145E+01	1.028E-02
1.150E-03	4.653E-04	1.305E+01	5.943E+02	6.162E-05	2.196E+01	1.059E-02
1.209E-03	4.930E-04	1.335E+01	5.943E+02	6.529E-05	2.246E+01	1.090E-02
1.269E-03	5.183E-04	1.320E+01	5.943E+02	6.865E-05	2.221E+01	1.121E-02
1.329E-03	5.437E-04	1.320E+01	5.943E+02	7.201E-05	2.221E+01	1.246E-02
1.388E-03	5.690E-04	1.305E+01	5.943E+02	7.537E-05	2.196E+01	1.495E-02
1.414E-03	5.944E-04	1.290E+01	5.943E+02	7.872E-05	2.170E+01	1.495E-02
1.439E-03	6.197E-04	1.290E+01	5.943E+02	8.208E-05	2.170E+01	1.619E-02
1.464E-03	6.451E-04	1.290E+01	5.943E+02	8.544E-05	2.170E+01	1.744E-02
1.490E-03	6.704E-04	1.170E+01	5.943E+02	8.880E-05	1.969E+01	1.993E-02
1.515E-03	6.958E-04	1.035E+01	5.943E+02	9.216E-05	1.741E+01	2.118E-02
1.540E-03	7.211E-04	8.700E+00	5.943E+02	9.551E-05	1.464E+01	2.491E-02
1.566E-03	7.465E-04	7.350E+00	5.943E+02	9.887E-05	1.237E+01	2.616E-02
1.591E-03	7.718E-04	6.600E+00	5.943E+02	1.022E-04	1.110E+01	2.740E-02

Appendix 11: Publication

Largeau, M.A.,Mutuku, R. and Thuo, J. (2018) Effect of Iron Powder (Fe2O) on Strength, Workability, and Porosity of the Binary Blended Concrete. Open Journal of Civil Engineering, 8, 411-425.

https://doi.org/10.4236/ojce.2018.84029